

Minimax Optimal Estimation of Stability Under Distribution Shift

Hongseok Namkoong^a Yuanzhe Ma^{b1} Peter W. Glynn^c

Decision, Risk, and Operations Division^a, Department of Industrial Engineering and Operations Research^b, and Management Science and Engineering^c

Columbia University^{a,b} Stanford University^c

namkoong@gsb.columbia.edu, ym2865@columbia.edu, glynn@stanford.edu

Abstract

The performance of decision policies and prediction models often deteriorates when applied to environments different from the ones seen during training. To ensure reliable operation, we analyze the *stability* of a system under distribution shift, which is defined as the smallest change in the underlying environment that causes the system’s performance to deteriorate beyond a permissible threshold. In contrast to standard tail risk measures and distributionally robust losses that require the specification of a plausible magnitude of distribution shift, the stability measure is defined in terms of a more intuitive quantity: the level of acceptable performance degradation. We develop a minimax optimal estimator of stability and analyze its convergence rate, which exhibits a fundamental phase shift behavior. Our characterization of the minimax convergence rate shows that evaluating stability against large performance degradation incurs a statistical cost. Empirically, we demonstrate the practical utility of our stability framework by using it to compare system designs on problems where robustness to distribution shift is critical.

1 Introduction

Distribution shift is a universal challenge in data-driven decision-making. Distribution shift can occur because data is often collected from a limited number of sources [107], marginalized groups are underrepresented [22], and decision policies operate in non-stationary environments [87]. On distributions different from that of the training data, the performance of decision policies and prediction models have been observed to deteriorate across a wide range of applications. Economic and healthcare policies must remain valid over space and time, but their external validity is often called into question [1, 135, 12, 125, 34]. Despite tremendous recent progress in machine learning systems, prediction models perform poorly under distribution shifts in healthcare [96, 10, 157, 21, 153], loan approval [65], wildlife conservation [13], and education [3]. For example, EPIC’s proprietary sepsis risk assessment model—currently deployed at hundreds of hospitals across the nation—has recently been found to perform “substantially worse” than the vendor’s claims [153].

Standard methods that evaluate average-case performance cannot ensure stable performance over unanticipated distribution shifts. As an example, consider a binary classification problem where the goal is to predict whether an individual is utilizing healthcare resources based on a set of rich individual-level covariates. We discuss the problem in detail in Section 5.2 and discuss how such classifiers can inform policy-making for low-income individuals. By

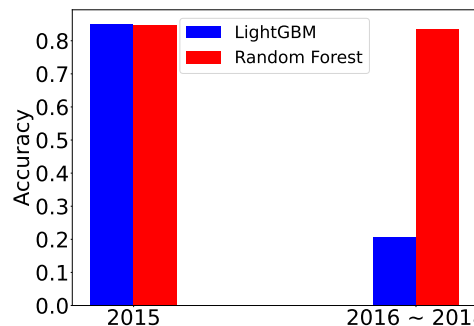


Figure 1. Models with initially near-identical average-case performance exhibit different accuracy over time.

¹HN and YM equally contributed to this work.

simulating an analyst *in 2015*, we use popular machine learning packages—gradient-boosted trees from LightGBM and random forests from scikitlearn—to train two classification models. While the two models achieve near-identical average-case performance on out-of-sample data from 2015 (Figure 1), their performance diverges dramatically in subsequent years. D’Amour et al. [32] recently observed a similar phenomenon across a wide range of prediction scenarios employed at Google.

To ensure the effectiveness of decision policies and prediction models, they must be rigorously tested before deployment. Toward this goal, we analyze the *stability* of a system under distribution shifts. For a given random cost function denoted by R , we consider an analyst who has access to i.i.d. scenarios with associated costs $R_1, \dots, R_n \stackrel{\text{iid}}{\sim} P$. For a chosen level of permissible performance degradation y , we define the *stability* of the system as the smallest distribution shift in the underlying environment that deteriorates performance above the threshold y . In stochastic control or reinforcement learning, the cost function R is often defined as the cumulative cost over a sample path; see Section 5.1 for a queueing example. In supervised learning contexts, the cost function R may be defined as the expected prediction error given a set of variables whose distributions may change over space and time; see Section 5.2 for an illustration on the healthcare example depicted in Figure 1.

We use the Kullback-Leibler (KL) divergence to quantify the notion of closeness between probability distributions. For a σ -finite measure μ such that $Q, P \ll \mu$, the KL divergence is

$$D_{\text{kl}}(Q\|P) := \mathbb{E}_Q \left[\log \frac{dQ/d\mu}{dP/d\mu} \right].$$

If Q is not absolutely continuous with respect to P , we have $D_{\text{kl}}(Q\|P) = \infty$. Formally, the stability $I_y(P)$ at threshold $y \geq \mathbb{E}_P[R]$ is defined as

$$I_y(P) := \inf_Q \{D_{\text{kl}}(Q\|P) : \mathbb{E}_Q[R] \geq y\}. \tag{1.1}$$

For simplicity, we omit the dependence on the threshold y and often write $I(P)$ or I . As we detail in Section 2, a well-known dual reformulation of the minimization problem (1.1) [38, Theorem 5.2] shows the optimal solution Q^* —the smallest adversarial distribution shift—is given by an exponential tilt $\frac{dQ^*}{dP} \propto \exp(\lambda^* R)$, where λ^* is the optimal dual variable that grows with y . Thus, the stability $I_y(P)$ measures the tail performance of the data-generating system P around the threshold y , and was proposed by Lemaitre et al. [97], Bachoc et al. [9].

Comparisons of tail risk across multiple system designs are meaningful insofar as the risk criterion is interpretable. There is a significant body of work on tail risk measures, e.g., coherent risk measures [5, 119, 35, 118] and other axiomatic definitions of tail risk [127, 120], and distributionally robust losses [15, 88, 116, 99, 144, 50] that consider worst-case performance over a pre-defined set of distributions. The two notions are closely related through duality [118, 131]. Since the evaluation of tail risk requires the modeler to postulate a magnitude of anticipated distribution shift, a plausible choice remains one of the biggest challenges in operationalizing notions of tail risk.

The stability measure (1.1) provides a complementary approach by comparing the stability of the system for a chosen threshold y in the *cost scale*. This approach is more intuitive and interpretable than setting a specific magnitude of distribution shift, such as $D_{\text{kl}}(Q\|P) \leq \rho$. It is often easier for analysts and engineers to decide on a tolerable amount of monetary loss or prediction error based on past data and domain knowledge when using the cost scale. While it is evident that no class of criteria is uniformly dominant, we highlight interpretability as a key advantage of the stability measure. A similar high-level approach is common in causal inference research where

through sensitivity analysis, researchers analyze the amount of unobserved confounding required to challenge the conclusion of an observational study [123, 124, 154]. For example, the finding that smoking causes lung cancer was considered credible because it would require an unrealistic amount of unobserved confounding (e.g., unrecorded hormone) to call the findings of the study into question [24]. Conceptually, our approach draws a parallel by analyzing how much distribution shift is required to deteriorate system performance to an intolerable degree.

Main contributions To build intuition, we begin with a dual reformulation of the infimum problem (1.1) in Section 2. We make concrete how the stability measure (1.1) is related to the tail probability of the cost R . Because committing to a plausible magnitude of distribution shift can be challenging, we study statistical estimation of stability $I_y(P)$ using i.i.d. observations $R_i \stackrel{\text{iid}}{\sim} P$ from the data-generating distribution P . Our main theoretical results characterize the finite sample minimax rate of convergence, which quantifies the fundamental rate at which $I_y(P)$ can be estimated based on n observations. Our finite sample results complement prior asymptotic convergence results for \hat{I}_n that assume a fixed data-generating distribution P [48, 28, 42, 43, 121].

Finite sample minimax rates are often considered overly conservative as it characterize the worst-case performance over a class of data-generating distributions

$$\mathfrak{M}_n := \inf_{\hat{I}_n} \sup_{P \in \mathcal{P}} \mathbb{E}_P \left| \hat{I}_n - I_y(P) \right|,$$

where the outer infimum is over all estimators—measurable functions of the data R_1, \dots, R_n —and the inner supremum is over data-generating distributions. (This set is not to be confused with possible distribution shifts we consider in our estimand (1.1).) To overcome this limitation and provide sharp insights, our analysis considers an highly restricted set of data-generating distributions. This allows us to characterize how the tail behavior of R impacts estimability of stability.

We crystallize our mathematical insight by studying random variables R with varying tail behavior. To maximize clarity in our theory, we characterize the minimax rate \mathfrak{M}_n for random variables with Gamma-like tails with $\mathbb{P}(R \geq t) \approx e^{-\sigma t}$ up to polynomial terms, where $\sigma = \inf\{\lambda : \mathbb{E}[e^{\lambda R}] = \infty\}$ is the abscissa of convergence. Our main results establish

$$\mathfrak{M}_n = \inf_{\hat{I}_n} \sup_{P \in \mathcal{P}} \mathbb{E}_P \left| \hat{I}_n - I_y(P) \right| \asymp n^{-\left(\frac{1}{2} \wedge \frac{\sigma}{\sigma_y}\right)}, \quad (1.2)$$

where \asymp notation hides constants that depend on σ and y , as well as polylogarithmic factors in n . In the formal results we present in Sections 3 and 4, we provide stronger results on the probability of error rather than expected estimation error. Our focus on Gamma-like tails allows a sharp characterization of how statistical difficulty depends on different tail behaviors, providing almost an instance-specific understanding.

To upper bound the minimax rate \mathfrak{M}_n , we focus on a simple plug-in estimator \hat{I}_n of the dual representation of $I_y(P)$ (see definition (2.3) to come). In Section 3, we prove that \hat{I}_n converges at a rate that depends on both the optimal dual variable and the abscissa of convergence $\sigma = \inf\{\lambda : \mathbb{E}[e^{\lambda R}] = \infty\}$. Our results show a phase transition in the convergence rate (1.2), which simultaneously depends on the

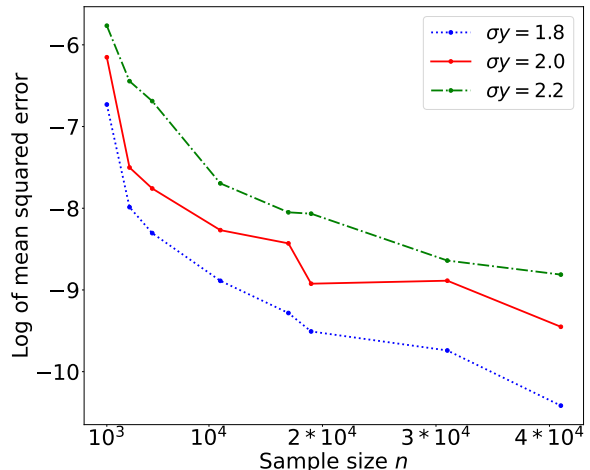


Figure 2. Mean squared error of \hat{I}_n (over 40 runs) with $P = \text{Exp}(\sigma)$, $\sigma \in \{0.9, 1, 1.1\}$ and a fixed threshold $y = 2$.

threshold y and the abscissa of convergence

$$\sigma = \inf\{\lambda : \mathbb{E}[e^{\lambda R}] = \infty\}. \quad (1.3)$$

For large values of y relative to σ , estimation becomes difficult as the stability measure increasingly focuses on the tails of $R \sim P$. We illustrate the degradation in convergence in Figure 2.

Our fundamental hardness results in Section 4 show that the pessimistic convergence rate is unavoidable for large values of y . This is surprising because we focus on a small set \mathcal{P} of data-generating distributions in the minimax risk (1.2) that exhibit Gamma-like tail behavior with a *fixed abscissa of convergence* σ (see Definition 1). When we consider distributions with different abscissas of convergence, it can be shown that the convergence rate further degrades to $\Omega_p(1/\log n)$. To our knowledge, our bounds are the first theoretical characterization of the fundamental difficulty in estimating $I_y(P)$, showing that *no statistical estimator* can avoid the degradation depicted in Figure 2. The rate (1.2) also makes clear how our focus on Gamma-like tails sharply characterizes the relationship between statistical efficiency and the tail behavior of R . In particular, for light-tailed random variables ($\sigma = \infty$), we do not observe a shape transition and recover simply the usual parametric rate. (See Corollaries 1 and 2 for formal statements.)

In Section 5, we empirically demonstrate how stability against a cost threshold y can provide practical assessments of system performance under potential distribution shift. On two problems where it is critical to maintain performance under distribution shift, we illustrate how the stability measure (1.1) differentiates between reliable vs. fragile designs. We then evaluate the performance of different system designs under both real and simulated distribution shifts, and show that the designs identified as the most stable according to our measure (1.1) are able to maintain good performance across a range of scenarios.

Related work Stability and robustness are central topics of interest for multiple scientific communities. We give a necessarily abridged review in the context of our work. In stochastic simulation, sensitivity analysis methods evaluate how performance measures (“outputs”) are affected by changes in the input variables [133, 90]. *Local* sensitivity analysis aims to quantify changes in the output induced by small perturbations in the input parameters [81]. See Glasserman [54, Ch. 7] and Asmussen and Glynn [7, Ch. 7] for a primer on derivative estimation in simulation settings. In finance, estimation of such local sensitivity is used to hedge against changes in the environment (e.g., price uncertainty). *Global* sensitivity analysis studies how input variability propagates to output variability. Many authors have used conditional variances to attribute the part of output variance due to variability in different subsets of the input [73, 129, 113, 134, 97]. Relatedly in robust satisficing [104], one allows the objective $\mathbb{E}_{Z \sim P} f(x, Z)$ to deviate from a given target when the underlying environment P changes, which is different to our setting. The fragility is defined as the worst expected degradation of the objective normalized by the change in P . In contrast, our notion of stability directly measures the least amount of perturbation required to make the loss intolerable.

Another related stream of work analyzes the local sensitivity of an output against *distributional uncertainty and model misspecification* [55, 89, 91, 92, 56, 58]. These works typically analyze the worst-case performance under infinitesimally small distribution shifts. By analyzing distributional variations induced by statistical uncertainty, a number of authors have recently proposed confidence intervals based on worst-case local sensitivity [93, 53, 16, 41]. In the context of the stability

measure (1.1), analyzing the impact of small distribution shifts is related to the limit $y \downarrow \mathbb{E}_P[R]$. In contrast, coherent risk measures and distributionally robust objectives measure the worst-case performance under a fixed ambiguity set of distribution shifts [118, 131, 80, 99]. As we are similarly concerned with stability against changes in the underlying environment, our main theoretical analysis studies a phase shift behavior for large values of y .

Reproducibility and stability is a critical concern in statistics [100, 156, 136, 111] and more generally, scientific research [78]. Classical robust statistics approaches [76, 108, 77] develop techniques (e.g., leverage score, breakdown point, influence function) to understand stability against sample outliers or sample removal [19, 49, 110]—as opposed to distribution shifts as in our work. In a recent work, Gupta and Rothenhäusler [63] introduced the s -value, a notion of stability similar to ours in the context of statistical inference. They propose a new paradigm of statistical inference and hypothesis testing centered around stability under distribution shifts. On the other hand, this work focuses on operational scenarios involving automated decision policies and prediction models and theoretically characterizes the finite sample minimax rate (1.2).

Although we take the data-generating distribution P as given, our approach is most effective when P contains diverse observations. Our framework is thus complementary to design-based perspectives in statistics and machine learning that aim to maximize heterogeneity in data. The burgeoning direction includes efforts to benchmark machine learning models across distribution shifts [128, 4, 86] and multi-site data collection in experimental design [25, 11, 52, 34, 139, 138].

2 Stability

The stability measure (1.1) assesses the smallest distribution shift that causes a meaningful degradation in system performance, measured by the threshold value y . In this work, we use the Kullback-Leibler divergence to measure the magnitude of distribution shift, a notion of distance that enjoys invariance to affine transformations. The KL divergence is widely used across multiple fields, including robust control [66], maximum likelihood in exponential families [20], Bayesian statistical analysis [14], and hypothesis testing [27]. However, its main limitation is that $D_{\text{kl}}(Q\|P) = \infty$ when Q is not absolutely continuous with respect to P ; the stability measure (1.1) is thus only defined over distribution shifts Q whose support is contained in that of the data-generating distribution P . In practice, this restriction does not greatly limit the applicability of the stability measure, as we primarily focus on analyzing the stability of real-valued performance measures. In many cases, it is natural to model the data-generating distribution P as having a long, continuous support in \mathbb{R} as we illustrate in Section 5.

Dual reformulation We begin our discussion by understanding the stability measure (1.1) through its dual reformulation. Rewrite the primal problem in terms of likelihood ratios $L := \frac{dQ}{dP}$

$$I_y(P) := \inf_Q \{D_{\text{kl}}(Q\|P) : \mathbb{E}_Q[R] \geq y\} = \inf_{L \geq 0} \{\mathbb{E}_P[L \log L] : \mathbb{E}_P[LR] \geq y, \mathbb{E}_P[L] = 1\}, \quad (2.1)$$

where the final infimum is taken over measurable functions. Taking the dual over this final problem, we arrive at the following classical reformulation.

Lemma 1 (Donsker and Varadhan [38, Theorem 5.2]). *Let $R \sim P$ be a real-valued random variable. For every y with $\mathbb{E}_P[R] \leq y < \text{ess sup } R$,*

$$I_y(P) = \sup_{\lambda \in \mathbb{R}} \left\{ \lambda y - \log \mathbb{E}_P[e^{\lambda R}] \right\}. \quad (2.2)$$

Furthermore, if the supremum on the right-hand side is attained at λ^* , then $\lambda^* \geq 0$ and the distribution Q^* that achieves the infimum on the left-hand side satisfies $dQ^*(x) = \frac{e^{\lambda^* x} dP(x)}{\mathbb{E}_P[e^{\lambda^* R}]}, \forall x \in \mathbb{R}$.

Although this result is well-known, we give a proof based on modern duality theory in Section A.1 for completeness.

Both the primal and dual formulations provide insights into how $I_y(P)$ grows with y . In the primal (1.1), the constraint set grows smaller as the threshold y increases, whereas y appears directly in the dual objective (2.2) via the Lagrangian. From first-order optimality conditions, the dual optimum λ^* satisfies

$$\frac{\mathbb{E}_P[Re^{\lambda^* R}]}{\mathbb{E}_P[e^{\lambda^* R}]} = y,$$

where the left-hand side is the derivative of the cumulant generating function $\lambda \mapsto \log \mathbb{E}_P[e^{\lambda R}]$ evaluated at λ^* . Lemma 1 states that the corresponding primal optimum is given by the exponential tilt $\frac{dQ^*}{dP} \propto e^{\lambda^* R}$, which upweights tail instances of R . From the convexity of the dual objective, it is clear that λ^* grows with y ; equivalently, the primal optimum approaches the essential supremum of R as y grows.

Concretely, the dual reformulation (2.2) allows us to build intuition by yielding analytic expressions for the stability measure I for specific distributions.

Example 1 (Gaussian distribution): If $R \sim P = \mathbf{N}(\mu, s^2)$ and $y \geq \mu$, then $\lambda^*(P) = \frac{y-\mu}{s^2}$, $I_y(P) = \frac{(y-\mu)^2}{2s^2}$, and $Q^*(P) = \mathbf{N}(y, s^2)$. \diamond

Example 2 (Gamma distribution): If $R \sim P = \text{Gamma}(\alpha, \sigma)$ and $y \geq \frac{\alpha}{\sigma}$, then $\lambda^*(P) = \sigma - \frac{\alpha}{y}$, $I_y(P) = sy - 1 - \alpha \log(\frac{\alpha}{sy})$, and $Q^*(P) = \text{Gamma}(\alpha, \frac{\alpha}{y})$. \diamond

Statistical estimation We use the dual formulation (2.2) to estimate $I_y(P)$ without parametric assumptions. Parametric assumptions on P are unrealistic and restrictive in general, but we view them to be particularly problematic since they require considering a limited set of distribution shifts Q . Denoting by \hat{P}_n the empirical distribution over the data R_1, \dots, R_n , consider the empirical plug-in estimator

$$\hat{I}_n := \sup_{\lambda \in \mathbb{R}} \left\{ \lambda y - \log \mathbb{E}_{\hat{P}_n} [e^{\lambda R}] \right\}. \quad (2.3)$$

Compared to the primal (1.1) counterpart that involves high-dimensional optimization over probability measures, the dual plug-in is efficient to compute as it only requires a binary search in a single dimension. Our main theoretical results to come demonstrate the optimality of the dual plug-in estimator (2.3), and exactly characterize how estimation becomes more challenging as the threshold y grows.

To illustrate that the simple plug-in estimator \hat{I}_n is nearly optimal, we compare it with another natural estimator \tilde{I}_n (2.4) that is based on a kernel density estimator \tilde{P}_n for the density of R with the Gaussian kernel [141]:

$$\tilde{I}_n := \sup_{\lambda \in \mathbb{R}} \left\{ \lambda y - \log \mathbb{E}_{\tilde{P}_n} [e^{\lambda R}] \right\}. \quad (2.4)$$

In Figure 3, we note that \tilde{I}_n converges at a much slower rate compared to \hat{I}_n .

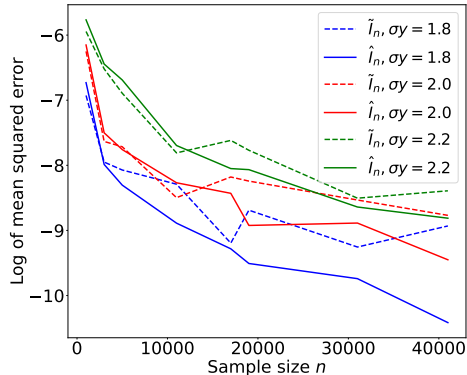


Figure 3. Mean squared error of \hat{I}_n and \tilde{I}_n (over 40 runs) with $P = \text{Exp}(\sigma)$, $\sigma \in \{0.9, 1, 1.1\}$ and a fixed threshold $y = 2$, here for \tilde{I}_n we choose the Gaussian kernel function with bandwidth $h = 0.1$

Connections to large deviations theory The dual reformulation (2.2) suggests our stability measure has deep connections to large deviations theory [36, 37, 45], which has a wide range of applications, including queueing theory, insurance mathematics, finance, and statistical mechanics [149, 6, 45, 140]. To illustrate the connection concretely, let $R_1, \dots, R_n \sim P$ be an i.i.d. sequence of random variables. Consider estimating the deviations probability of a random walk $S_m := \sum_{i=1}^m R_i$

$$p_m := \mathbb{P}(S_m/m \in A) \quad \text{where } A \subset \mathbb{R} \text{ s.t. } \mathbb{E}[R] \notin A. \quad (2.5)$$

Large deviations theory [36] shows the approximation

$$p_m \approx e^{-m \inf_{y \in \text{cl}(A)} I_y(P)},$$

where the stability measure $I_y(P)$ is alternatively called the large deviations rate function. Our choice of notation is intentional to make this connection explicit.

Since $y \mapsto I_y(P)$ is nondecreasing on $[\mathbb{E}_P[R], \infty)$, there is no real loss of generality in restricting attention to one-sided intervals $A = [y, \infty)$ for a fixed $y \geq \mathbb{E}_P[R]$. In particular, Cramer’s theorem [7, Ch VI. Lemma 2.8] shows

$$p_m = \mathbb{P}(S_m \geq my) = \exp(-mI_y(P) + \Theta(\sqrt{m})). \quad (2.6)$$

As a product of this connection, the main statistical results we give in the sequel can be adapted to provide minimax convergence rates on the deviations probability (2.5). While these results appear new to the literature, we omit them for brevity.

Extensions While a natural and classical starting point (e.g., [97]), our focus on the KL divergence is admittedly somewhat arbitrary. We provide duality results for alternative metrics in Appendix A.1 and leave as future work a proper comparison *between* different stability measures. In contrast to distributionally robust formulations that consider the KL divergence across the *joint distribution on the entire data*, the notions of stability we consider only concern the single-dimensional random variable R . As a result, we conjecture that the choice of the notion of distance in the stability measure is less important than in DRO.

3 Convergence results

In the following two sections, we present our main theoretical contributions, which characterize the minimax rate of convergence for estimating the stability measure (1.1). We take a two-pronged approach, where we first establish finite sample convergence guarantees for the empirical plug-in estimator for the dual formulation (2.2)

$$\widehat{I}_n := \sup_{\lambda \in \mathbb{R}} \left\{ \lambda y - \log \mathbb{E}_{\widehat{P}_n} [e^{\lambda R}] \right\}.$$

Without imposing parametric assumptions on the distribution of R , we characterize how the convergence rate depends on the threshold y and the abscissa of convergence $\sigma = \inf\{\lambda : \mathbb{E}[e^{\lambda R}] = \infty\}$. In combination with hardness bounds we give in the next section, our results show that the dual plug-in estimator \widehat{I}_n enjoys the best achievable finite sample convergence rate uniformly over a class of distributions. In contrast, direct plug-in approaches based on nonparametric estimators of P converge at a slow nonparametric rate that depends exponentially on the smoothness of the density of R [147].

Our main result in this section quantifies the phase shift behavior in the convergence rate. As our goal is to obtain convergence guarantees uniform over the underlying distribution P , we consider a class of distributions such that the optimal dual solution is bounded by some specified upper bound $\bar{\lambda}$

$$\lambda^*(P) = \operatorname{argmax}_{\lambda} \left\{ \lambda y - \log \mathbb{E}_P [e^{\lambda R}] \right\} \leq \bar{\lambda}.$$

Our proof uses chaining techniques [142, Ch 2.2] to uniformly bound the empirical process $\lambda \mapsto \mathbb{E}_{\widehat{P}_n} [e^{\lambda R}] - \mathbb{E}_P [e^{\lambda R}]$ over the interval $[0, \bar{\lambda}]$, which in turn bounds the estimation error $\widehat{I}_n - I$.

Our main finite sample result makes explicit the distribution-dependent constants that govern convergence behavior and thus allow proving uniform convergence results. Our upper bound results (Theorems 2, 3) follow as corollaries of the following theorem.

Theorem 1. *Let $\bar{\lambda} > 0$ be a fixed constant with $\lambda^*(P) \leq \bar{\lambda}$ and let β satisfy $1 < \beta \leq \min\{2, \frac{\sigma}{\bar{\lambda}}\}$ where σ is the abscissa of convergence (1.3). There is a universal constant $K > 0$ such that*

$$\mathbb{P} \left(\left| \widehat{I}_n - I(P) \right| \geq K \left(\frac{1}{\delta} \right)^{\frac{1}{\beta}} \bar{\lambda} \left(\mathbb{E}_P [|R|^\beta e^{\bar{\lambda} \beta R}] \right)^{\frac{1}{\beta}} n^{\frac{1}{\beta} - 1} \right) \leq \delta. \quad (3.1)$$

See Section B for the proof.

Recalling the definition of the abscissa of convergence (1.3), $e^{\bar{\lambda} R}$ has at most $(\sigma/\bar{\lambda})$ number of moments. This observation uncovers a natural phase shift phenomenon for the dual plug-in estimator, as we empirically observed in Figure 2. When $\sigma/\bar{\lambda} > 2$, we show the existence of second moments allows the dual plug-in to achieve the parametric rate $O_p(n^{-1/2})$. On the other hand, consider the case when $\sigma/\bar{\lambda} \leq 2$. Since the dual solution λ^* grows with y —this is easy to verify using first-order conditions— $\sigma/\bar{\lambda} \leq 2$ implies the threshold y is large relative to the abscissa of convergence σ . Since $e^{\lambda^* R}$ may not have a second moment, in this case, we prove the convergence rate deteriorates to $O_p(n^{\bar{\lambda}/\sigma - 1})$, which becomes worse as y becomes larger. Treating these two cases separately, we refer to $\sigma/\bar{\lambda} \leq 2$ and $\sigma/\bar{\lambda} > 2$ as the large and moderate deviations regime respectively.

Concretely, we study the minimax rate of convergence for estimating $I_y(P)$ over a natural class of distributions that exhibit Gamma-like tail behavior. Since Theorem 1 gives convergence results

that explicitly depend on the underlying data-generating distribution P , we take worst-case rates over this class of distributions with Gamma-like tails.

Definition 1. For σ, y, α with $\sigma y > 1$ and $\alpha \in (0, 1)$, $\mathcal{P}_{\sigma, y, \alpha}$ is the class of distributions satisfying the following conditions.

1. $R \geq 0$ and $\mathbb{E}_P[e^{\sigma R}] = \infty$.
2. $\mathbb{E}_P[e^{\lambda R}] \leq \frac{\sigma}{\sigma - \lambda}$ for $0 \leq \lambda < \sigma$ and $\mathbb{E}_P[R] \leq \frac{1}{\sigma}$.
3. $\lambda^*(P) = \operatorname{argmax}_{\lambda} \{ \lambda y - \log \mathbb{E}_P[e^{\lambda R}] \} \leq \sigma - \frac{\alpha}{y} =: \bar{\lambda}$.

The condition $R \geq 0$ has no real significance other than simplifying the calculations in the upper bound; the condition merely provides a range on which R is anchored in. As we showcase in our empirical demonstrations, the translation-invariant property of the stability measure allows translating the cost R and the threshold y by a constant to ensure nonnegativity. We assume $\sigma y > 1$ since $\lambda^*(P) = 0$ and $I(P) = 0$ for $P = \operatorname{Exp}(\sigma) \in \mathcal{P}_{\sigma, y, \alpha}$ with $\sigma y \leq 1$. The condition $\mathbb{E}_P[R] \leq \frac{1}{\sigma}$ ensures $\mathbb{E}_P[R] \leq \frac{1}{\sigma} < y$.

Conditions 1, 2 restrict $\mathcal{P}_{\sigma, y, \alpha}$ to have Gamma-like tails so that $\mathbb{P}(R \geq t)$ decays like $e^{-\sigma t}$ up to polynomial terms. To contextualize Condition 3, consider $R \sim P_0 = \operatorname{Gamma}(\alpha, \sigma)$, which has $\lambda^*(P_0) = \sigma - \alpha/y$. The final condition thus considers distributions with the optimal exponential tilting factor $\lambda^*(P)$ bounded by that of the Gamma distribution with shape α and rate σ . To unpack the condition further, denote by κ_P the cumulant generating function, $\kappa_P(\lambda) = \log \mathbb{E}_P[e^{\lambda R}]$, and recall $\lambda^*(P)$ satisfies $\kappa'_P(\lambda^*(P)) = y$ from first-order optimality conditions. Since $\kappa_P(\cdot)$ is convex, $\kappa'_P(\lambda) = \mathbb{E}_P[Re^{\lambda R}]/\mathbb{E}_P[e^{\lambda R}]$ is non-decreasing in λ . Hence, Condition 3 is equivalent to

$$\mathbb{E}_P[Re^{(\sigma - \alpha/y)R}] \geq y \mathbb{E}_P[e^{(\sigma - \alpha/y)R}], \quad (3.2)$$

which roughly implies R has heavy enough tails. When $R \sim P_0 = \operatorname{Gamma}(\alpha, \sigma)$, equality holds in the above display (3.2).

We first consider the large deviations regime where $\sigma y \geq 2\alpha$. Our convergence result explicitly quantifies how the statistical error of the dual plug-in \hat{I}_n degrades with y .

Theorem 2. Fix $\alpha \in (0, 1)$. Let $\sigma y \geq 2\alpha$ and $\sigma y > 1$. There is a universal constant $K > 0$ such that for any $\delta \in (0, 1)$ and $n \geq 8$,

$$\sup_{P \in \mathcal{P}_{\sigma, y, \alpha}} \mathbb{P} \left(\left| \hat{I}_n - I(P) \right| \geq K \left(1 - \frac{\alpha}{\sigma y} \right) \left(\frac{1}{\delta} \right)^{2(1 - \frac{\alpha}{\sigma y})} \left(4 \left(1 - \frac{\alpha}{\sigma y} \right) \log n \right)^{1 + 2(1 - \frac{\alpha}{\sigma y})} n^{-\frac{\alpha}{\sigma y}} \right) \leq \delta. \quad (3.3)$$

See Section B.2 for the proof.

On the other hand, in the moderate deviations regime where $\sigma y < 2\alpha$, the dual plug-in estimator \hat{I}_n achieves uniform parametric rates. This is in contrast to the primal plug-in estimator, which suffers nonparametric rates even in this regime due to the difficulty of estimating densities.

Theorem 3. Fix $\alpha \in (0, 1)$. Let $1 < \sigma y < 2\alpha$. There is a universal constant $K > 0$ such that for any $\delta \in (0, 1)$,

$$\sup_{P \in \mathcal{P}_{\sigma, y, \alpha}} \mathbb{P} \left(\left| \hat{I}_n - I(P) \right| \geq K \left(\frac{1}{\delta} \right)^{\frac{1}{2}} \left(\frac{\sigma y}{\alpha - \frac{\sigma y}{2}} \right)^{\frac{1}{2}} \frac{\sigma y - \alpha}{\alpha - \frac{\sigma y}{2}} n^{-\frac{1}{2}} \right) \leq \delta. \quad (3.4)$$

See Section B.3 for the proof. Using the identity $\mathbb{E}[X] = \int_0^\infty \mathbb{P}(X \geq x) dx$ for a nonnegative random variable X , our probability bounds can be transformed to give upper bounds on the expected absolute error as we initially outlined in the display (1.2).

To consider a broader class of distributions, we extend Definition 1 by relaxing Condition 2.

Definition 2. For $m \geq 1, m \in \mathbb{N}_+, \sigma, y, \alpha$ with $\sigma y > m, \alpha \in (0, 1), \mathcal{P}_{\sigma, y, \alpha, m}$ is the class of distributions satisfying the following conditions.

1. $R \geq 0$ and $\mathbb{E}_P[e^{\sigma R}] = \infty$.
2. $\mathbb{E}_P[e^{\lambda R}] \leq \left(\frac{\sigma}{\sigma - \lambda}\right)^m$ for $0 \leq \lambda < \sigma$ and $\mathbb{E}_P[R] \leq \frac{m}{\sigma}$.
3. $\lambda^*(P) = \operatorname{argmax}_\lambda \{\lambda y - \log \mathbb{E}_P[e^{\lambda R}]\} \leq \sigma - \frac{\alpha}{y} =: \bar{\lambda}$.

The condition $\mathbb{E}_P[R] \leq \frac{m}{\sigma}$ ensures $\mathbb{E}_P[R] \leq \frac{m}{\sigma} < y$ for any $P \in \mathcal{P}_{\sigma, y, \alpha, m}$. Condition 2 restricts all distributions in $\mathcal{P}_{\sigma, y, \alpha, m}$ to have a lighter tail compared to $\text{Gamma}(m, \sigma)$, while Condition 3 requires P to have a heavier tail compared to $\text{Gamma}(\alpha, \sigma)$. Thus, $\text{Gamma}(k, \sigma) \in \mathcal{P}_{\sigma, y, \alpha, m}$ for all $k \in [\alpha, m]$.

Recalling we assume $\sigma y > m$ in Definition 2, the inequality $\sigma y > m > 2\alpha$ always holds for $\alpha < \frac{1}{2}$ and therefore we only have the large deviations regime in this case. We have the upper bound result that is similar to Theorem 2, which we prove in Section B.4.

Theorem 4. Fix $\alpha \in (0, 1)$. Let $\sigma y > m > 2\alpha$. There is a universal constant $K > 0$ such that for any $\delta \in (0, 1)$ and $n \geq 8$,

$$\sup_{P \in \mathcal{P}_{\sigma, y, \alpha, m}} \mathbb{P} \left(\left| \widehat{I}_n - I(P) \right| \geq K \left(1 - \frac{\alpha}{\sigma y}\right) \left(\frac{1}{\delta}\right)^{2(1 - \frac{\alpha}{\sigma y})} \left(4 \left(1 - \frac{\alpha}{\sigma y}\right) \log n\right)^{1 + 2m(1 - \frac{\alpha}{\sigma y})} n^{-\frac{\alpha}{\sigma y}} \right) \leq \delta. \quad (3.5)$$

We can also extend the results in this section to light-tailed random variables. Letting $\sigma \rightarrow \infty$ in Theorem 1, we obtain the following result.

Corollary 1. Let $\bar{\lambda}$ be any fixed constant with $\lambda^*(P) \leq \bar{\lambda}$ and assume $\mathbb{E}_P[e^{\lambda R}] < \infty$ for any λ . There exists a universal constant $K > 0$ such that

$$\mathbb{P} \left(\left| \widehat{I}_n - I(P) \right| \geq K \left(\frac{1}{\delta}\right)^{\frac{1}{2}} \bar{\lambda} \left(\mathbb{E}_P[|R|^2 e^{2\bar{\lambda} R}]\right)^{\frac{1}{2}} n^{-\frac{1}{2}} \right) \leq \delta. \quad (3.6)$$

Concretely, we study the class of light-tailed distributions $\mathcal{Q}_{\bar{\lambda}, y}$ defined below.

Definition 3. For $\bar{\lambda} > 0$ and $y, \mathcal{Q}_{\bar{\lambda}, y}$ is the class of distributions satisfying the following conditions.

1. $\mathbb{E}_P[e^{\lambda R}] < \infty$ for any λ .
2. $\lambda_y^*(P) = \operatorname{argmax}_\lambda \{\lambda y - \log \mathbb{E}_P[e^{\lambda R}]\} \leq \bar{\lambda}$.

Corollary 1 implies the standard $1/\sqrt{n}$ convergence rate

$$\sup_{P \in \mathcal{Q}_{\bar{\lambda}, y}} \mathbb{P} \left(\left| \widehat{I}_n(R_1^n) - I_y(P) \right| \geq K \left(\frac{1}{\delta} \right)^{\frac{1}{2}} \frac{1}{\sqrt{n}} \right) \leq \delta,$$

where K is some constant that depends on $\bar{\lambda}, y$. For fixed $\bar{\lambda}$ and y , we can show (see Section B.5) that $\mathcal{Q}_{\bar{\lambda}, y}$ contains the following sub-Gaussian distributions:

$$\left\{ \mathbf{N}(\mu, s^2) : \frac{y - \mu}{s^2} \leq \bar{\lambda} \right\}, \left\{ \text{Ber}(p) : p \geq \frac{y}{e^{\bar{\lambda}} - y(e^{\bar{\lambda}} - 1)} \right\}, \left\{ \text{Uni}(a, b) : \frac{b - a}{b - y} \leq \bar{\lambda} \right\} \subset \mathcal{Q}_{\bar{\lambda}, y},$$

To further understand $\mathcal{Q}_{\bar{\lambda}, y}$, consider any light-tailed random variable $R \sim P$ with $y < \text{ess sup } R$, we can show that there exists $\tilde{\lambda}(y, P) < \infty$ such that $P \in \mathcal{Q}_{\tilde{\lambda}(y, P), y}$. This implies for any finite set of light-tailed distributions \mathcal{P} with $y \leq \text{ess sup } R$ for any $R \sim P \in \mathcal{P}$, we can find $\tilde{\lambda}(y, \mathcal{P})$ such that $\mathcal{P} \subseteq \mathcal{Q}_{\tilde{\lambda}(y, \mathcal{P}), y}$.

4 Fundamental hardness

We now provide lower bounds on the minimax risk (1.2) that complement our convergence results in the previous section (Theorems 2 and 3). Our lower bounds quantify the fundamental hardness of estimation and show that the plug-in estimator (2.3) achieves the optimal rate of convergence up to polylogarithmic factors. Unlike previous asymptotic results that consider a fixed data-generating distribution P [47], we consider a fixed finite sample size and quantify the difficulty of estimation over a class of data-generating distributions. As minimax lower bounds [145] can be overly pessimistic when considering a large set of data-generating distributions, we focus on the adapted class of distributions $\mathcal{P}_{\sigma, y, \alpha}$ that exhibit a particular Gamma-like tail behavior defined in Definition 1.

As an example of pessimistic hardness results when considering a large class of data-generating distributions, consider the case where we do not restrict distributions in $\mathcal{P}_{\sigma, y, \alpha}$ to have the same abscissa of convergence $\sigma = \inf\{\lambda : \mathbb{E}[e^{\lambda R}] = \infty\}$. So long as $\mathcal{P}_{\sigma, y, \alpha}$ just contains two distributions with tails decaying like $e^{-\sigma x}$ and $e^{-\sigma(1-1/\log n)x}$, we can show that no estimator of stability $I_y(P)$ can have expected estimation error better than $\Omega(1/\log n)$. Intuitively, this is due to the inherent difficulty in estimating σ , the abscissa of convergence. Since σ is the knife-edge determining the existence of the MGF, it is difficult to estimate: it is well known that the minimax rate for estimating σ is $\Theta_p(1/\log n)$ [64].

With this theoretical motivation in mind, we focus on the admissible setting where σ is fixed (Conditions 1, 2). We characterize a *tailored* notion of hardness adapted to the class $\mathcal{P}_{\sigma, y, \alpha}$, and show an unavoidable degradation from the parametric rate even over the restricted set of distributions with a fixed abscissa of convergence σ . The phase shift behavior $\tilde{\Theta}_p(n^{-(\frac{1}{2} \wedge \frac{\alpha}{\sigma y})})$ in our bound (1.2) is fundamental. Estimation becomes harder for large threshold values y , as well as for light-tailed distributions with higher σ . Although a priori counterintuitive, the latter scaling is natural since adverse events with large values of R occur more rarely for lighter-tailed distributions, and the stability measure is thus more difficult to estimate.

To prove our minimax lower bound, we use Le Cam's reduction from estimation to hypothesis testing [94, 95, 155]. Our information-theoretic approach constructs two distributions close in total variation distance—thus difficult to tell apart using finite samples—but sufficiently separated with respect to the stability $I(P)$. Although we state probabilistic minimax bounds for the estimation

error, their expectation counterparts can also be easily shown from our proofs. Following Section 3, we first focus on the large deviations regime, where we observe a degradation from the standard parametric rate.

Theorem 5. Fix $\alpha \in (\frac{1}{2}, 1)$ and $\delta \in (0, \frac{1}{2})$. Let $\sigma y \geq 2\alpha > 1$ and define $c = \frac{1}{2(1-2\delta)^2}$. If

$$\log cn \geq \max \left\{ \frac{\sigma y}{\alpha} \left(2 \log \frac{\log cn}{\sigma} + \log \left(\frac{4\sigma \left(\frac{\alpha}{y} \vee 1 \right)}{1-\alpha} \right) \right), \sigma y \left(\frac{2}{\alpha^2} \frac{\sigma y + 1}{\sigma y - 1} \vee \frac{2}{\alpha} \vee \frac{4}{\sigma y - 1} \right), \right. \\ \left. \frac{2\sigma \log 3(1 \vee \sigma^{-2})}{1-\alpha}, \sigma + 1, \frac{2}{1-\alpha} \right\},$$

$$\mathfrak{M}_n := \inf_{\hat{I}_n} \sup_{P \in \mathcal{P}_{\sigma, y, \alpha}} \mathbb{P} \left(\left| \hat{I}_n(R_1^n) - I(P) \right| \geq \left(\frac{\sigma y}{\log cn} \right)^{1-\alpha} \frac{\sigma y - 1}{4\Gamma(\alpha) e^{\frac{1}{\sigma y}} (\sigma y + 1) (\log cn - 1)} \left(\frac{1}{cn} \right)^{\frac{\alpha}{\sigma y}} \right) \geq \delta,$$

where the infimum is taken over the set of (R_1, \dots, R_n) -measurable functions.

Deferring a formal proof of Theorem 5 to Section C.1, we outline the main ideas below. We construct two distributions $P_1, P_2 \in \mathcal{P}_{\sigma, y, \alpha}$ that exhibit slightly different tail behaviors

$$f_1(x) \propto x^{\alpha + \frac{1}{\sigma x_0} - 1} e^{-\sigma x} \mathbf{1}\{x \geq 0\} \quad \text{and} \quad f_2(x) \propto \begin{cases} x^{\alpha + \frac{1}{\sigma x_0} - 1} e^{-\sigma x} & \text{if } 0 \leq x \leq x_0 \\ x^{-1} e^{-\sigma x} & \text{if } x > x_0 \end{cases}. \quad (4.1)$$

By selecting x_0 appropriately, we can show that samples from the two distributions are difficult to tell apart with probability at least δ , yet the stability measures $I(P_1)$ and $I(P_2)$ are at least $\tilde{\Omega}(n^{-\frac{\alpha}{\sigma y}})$ separated.

In the moderate deviations regime where $\sigma y < 2\alpha$, we can show that the minimax lower bound reduces to the usual parametric rate.

Theorem 6. Fix $\alpha \in (\frac{1}{2}, 1)$ and $\delta \in (0, \frac{1}{2})$. Let $1 < \sigma y < 2\alpha$. If

$$\log n \geq \max \left\{ 2 \left(\log \left(\frac{1}{(1-\alpha) \wedge (2-\sigma y)} \right) + \log 2(1-2\delta) + \log \sigma y \right), \sigma y \log 2 + \log 2(1-2\delta) \right\}, \\ \mathfrak{M}_n := \inf_{\hat{I}_n} \sup_{P \in \mathcal{P}_{\sigma, y, \alpha}} \mathbb{P} \left(\left| \hat{I}_n(R_1^n) - I(P) \right| \geq \frac{(\sigma y - 1)(1 - 2\delta)}{4\sqrt{n}} \right) \geq \delta.$$

Compared to the construction (4.1) for Theorem 5, the ‘‘hard examples’’ P_1 and P_2 take on a different shape when $\sigma y < 2\alpha$. In this regime, we consider a more standard example of two distributions that differ in their average-case behavior (when $x \leq x_0$) in our proof in Section C.3.

The lower bound results shown Theorems 5 and 6 still hold when we replace $P \in \mathcal{P}_{\sigma, y, \alpha}$ with $P \in \mathcal{P}_{\sigma, y, \alpha, m}$ introduced in Definition 2 since $\mathcal{P}_{\sigma, y, \alpha} \subseteq \mathcal{P}_{\sigma, y, \alpha, m}$ for any $m \geq 1$. Combining these with Theorem 4, we extend our main result (1.2) to the more general class of distributions $\mathcal{P}_{\sigma, y, \alpha, m}$:

$$\inf_{\hat{I}_n} \sup_{P \in \mathcal{P}_{\sigma, y, \alpha, m}} \mathbb{E}_P \left| \hat{I}_n - I_y(P) \right| \asymp n^{-\left(\frac{1}{2} \wedge \frac{\alpha}{\sigma y}\right)}.$$

We can also extend the main results in this section to random variables with light-tailed random variables. In this case, we recover the usual parametric rate. See Section C.4 for the proof.

Corollary 2. Fix $\bar{\lambda}, y$ such that $\mathcal{Q}_{\bar{\lambda}, y} \neq \emptyset$ and $\delta \in (0, \frac{1}{2})$. Define $c = 2(1 - 2\delta)$. If $n \geq \left(\frac{c}{\bar{\lambda}}\right)^2$,

$$\mathfrak{M}_n := \inf_{\hat{I}_n} \sup_{P \in \mathcal{Q}_{\bar{\lambda}, y}} \mathbb{P} \left(\left| \hat{I}_n(R_1^n) - I_y(P) \right| \geq \bar{\lambda} \frac{c}{2\sqrt{n}} \right) \geq \delta,$$

where the infimum is taken over the set of (R_1, \dots, R_n) -measurable functions.

5 Experiments

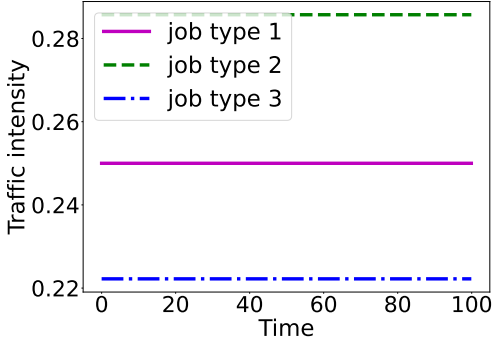
We empirically demonstrate our approach in two operational problems where it is critical to evaluate system stability prior to deployment. First, we study scheduling policies in queueing, where the modeler learns a scheduling policy based on a simulator and wishes to ensure the deployed policy maintains robust performance over multiple real-world environments. Second, we turn our attention to the empirical evaluation of prediction models. We study models trained to predict healthcare resource utilization based on past and present data. Since demographic distributions shift over time, we wish to ensure that predictive performance remains stable in the future. We adapt our proposed methodology to be less conservative by considering distribution shift only over a subset of covariates instead of the usual joint distribution shift over all randomness. This allows modeling more structured and realistic distribution shifts that occur in predictive modeling. In both scenarios, the proposed stability measure differentiates between brittle vs. robust models, in contrast to typical average-case performance metrics that do not account for tail performance. Our empirical study also highlights the limitation of the proposed approach and directions of future work.

5.1 Queueing systems

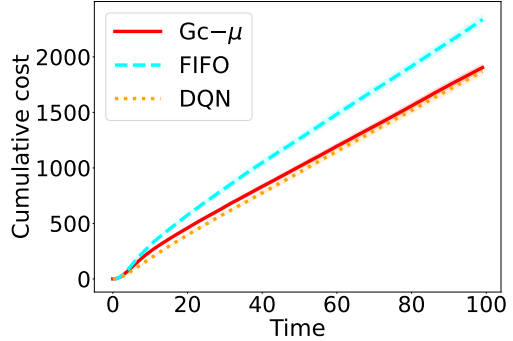
Managing congestion under resource constraints is a core goal in operations research [152]. Scheduling policies must maintain robust performance over varied distribution shifts that occur in real-world queueing systems [87, 59, 60, 44]. In contrast to typical simplifying assumptions in queueing theory, arrival distributions are often highly nonstationary [57], and demand surges are frequent [74]. Simultaneously, supply-side disruptions due to staffing difficulties [23, 51] are increasingly common, leading to nonstationary service rates.

We use a G/G/1 queue with multi-class jobs as the primary vehicle for modeling stochastic workloads, where we consider jobs that incur quadratic costs with sojourn time [143]. Solving for the optimal scheduling policy is intractable even for a single-server queue with a fixed arrival and service distribution due to the prohibitively large state/policy spaces [114]. We compare the stability of two approximation methods that take radically different approaches. First, we look to the classical heavy-traffic limit literature that designs effective policies under highly congested environments [67, 143, 150, 68, 106]. Under the tractable heavy-traffic diffusion limit, a simple index-based myopic policy—the generalized c - μ rule (Gc- μ)—is optimal for convex cost functions [143]. The Gc- μ rule is intuitive and does not require any arrival information: it serves jobs with the highest index calculated by the product of instantaneous cost and the service rate. It enjoys a natural adversarial robustness guarantee under demand surges, although its optimality is only guaranteed in the heavy-traffic limit.

As an alternative to the classical index-based policy, we study deep reinforcement learning (DRL) approaches to queueing. DRL methods have recently achieved remarkable success in games



(a) Traffic intensities $\rho(t) = \frac{\lambda(t)}{\mu(t)}$ representing arrival and service rates for each class.



(b) Average cumulative costs. Shaded regions denote $\pm 1.96 \times$ standard deviations.

Figure 4: Performance of policies on i.i.d. test data

and robotics [132, 62], and can heuristically solve the scheduling dynamic program through black-box function approximations. However, they are generally difficult to train reliably due to unbounded state spaces in queueing systems [146, 31]. They empirically exhibit high sensitivity to hyperparameters, implementation details, and even random seeds [72]. Although DRL methods require significant engineering effort and a large number of simulated samples to achieve good performance in practice, we demonstrate below that DRL approaches can effectively optimize queueing performance under a fixed system dynamics.

We consider a single-server multi-class queueing model operating in a finite time interval $[0, 100]$, which we implement using a custom discrete-event simulator. We consider three job types $j \in \mathcal{J} = \{1, 2, 3\}$ with independent interarrival times. Denote by $\lambda_j(t)$ and $\mu_j(t)$ the arrival and service rates and $\rho_j(t) = \frac{\lambda_j(t)}{\mu_j(t)}$ the traffic intensity at time t . We consider cost functions $C_j(x) = w_j x^2$ with $w_1 = 1, w_2 = 3, w_3 = 6$ where x is the time a job spent in the system. We focus on a scenario where the modeler has access to a calibrated simulator with independent inter-service times following an exponential distribution with mean $\frac{1}{\mu_j(t)}$ and independent interarrival distribution

$$\frac{1}{2} \text{Exp}(\lambda_j(t)) + \frac{1}{2} \left| \text{N} \left(0, \lambda_j(t)^{-2} \frac{\pi}{2} \right) \right|.$$

Following standard practice, we fix the training distribution to have stationary arrival and service rates.

We compare three different scheduling policies. As our first policy, letting $a_j(t)$ be the age of the oldest type j job at time t , the Gc- μ rule serves jobs with the highest value of $C'_j(a_j(t))\mu_j(t)$ (breaking ties arbitrarily). Since the Gc- μ rule only requires knowledge of service rates, we assume $\mu_j(\cdot)$ is known as it can easily be estimated from offline data. Second, we use a Q-learning method where we estimate the value function using a feedforward neural network (DQN; Deep Q-Networks [109]). Deferring implementation details to Section D.1, we note that since the DQN policy is finetuned to the particular simulation setting—itsself often calibrated from data—its robustness under distribution shift is of substantial concern. Finally, we consider the first-in-first-out (FIFO) policy as a simple benchmark.

On the training distribution with stationary arrival and service rates, we first evaluate the average cumulative cost under each policy over $n = 100,000$ sample paths. Since the DQN model was trained to optimize performance on this distribution, we observe it achieves the best average-

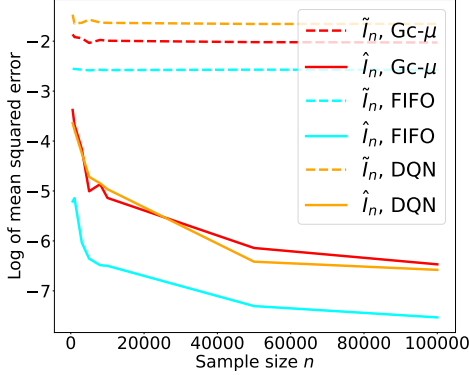


Figure 5. Mean squared error of \hat{I}_n (over 40 runs) for different policies with threshold $y = 3720.66$. Here for the KDE estimator \tilde{I}_n (2.4) we choose the Gaussian kernel function with bandwidth $h = 100$.

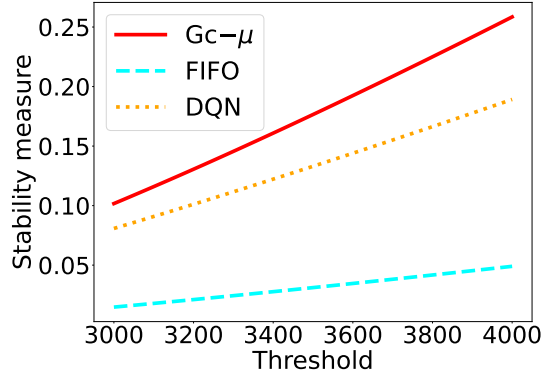


Figure 6. Stability \hat{I}_n for different policies over a set of thresholds

case performance in Figure 4. As distribution shifts and nonstationarities are common in practice [87, 59, 60, 44], we also evaluate the stability of each policy using the cumulative cost at the end of the horizon ($t = 100$). We first assess the validity of our estimation strategy. We again compare our estimator \hat{I}_n based on the dual reformulation (2.2) with the one based on kernel density estimation of R (2.4). Similar to Figure 2, in Figure 5, we analyze the convergence rate of different estimators. For all three decision policies, we observe that our dual-based estimator outperforms nonparametric counterparts by multiple orders of magnitude.

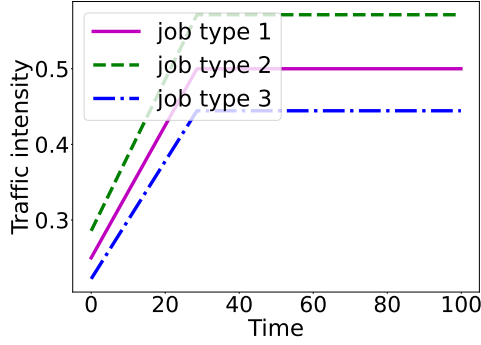
Next, we use our dual-based estimator to compare the stability of different decision policies. To set a common benchmark performance for all policies, we choose the threshold value y to be twice the mean of the average cumulative cost under the DQN policy. Despite choosing a threshold value that unfairly favors the DQN policy—as it had the lowest average cost—in Table 1 we observe that the Gc- μ rule exhibits the highest stability. To further examine whether Gc- μ rule is robust due to the choice of y , we compute \hat{I}_n over a wide range of thresholds, and in Figure 6, we see the gap in stability growing as y increases.

Policy	Stability \hat{I}_n	Average Cost
Gc- μ	0.21194	1928.72
DQN	0.15741	1861.79
FIFO	0.03887	2345.53

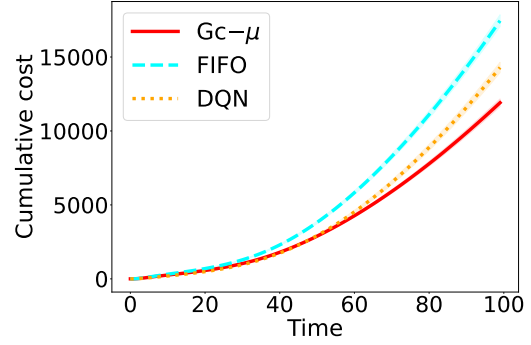
Table 1: Stability with threshold $y = 3720.66$

The proposed stability measure simulates worst-case distribution shifts by only using training data. To contextualize our findings, we simulate five concrete distribution shifts modeling different changes to arrival and service rates in the same family of distributions as above.

1. Arrival rates linearly increase to certain levels over time.
2. There is a sudden increase in arrival rates.
3. Service rates linearly decrease to certain levels over time.
4. Arrival rates linearly increase, and service rates linearly decrease to certain levels over time.
5. Arrival rates are cyclical (sinusoidal).

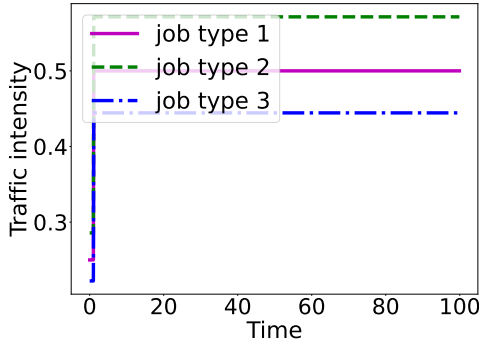


(a) Traffic intensities $\rho(t) = \frac{\lambda(t)}{\mu(t)}$ representing arrival and service rates for each class.

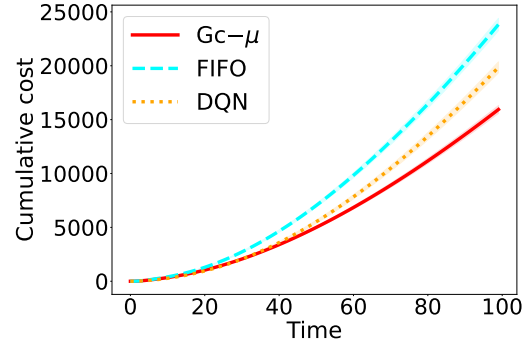


(b) Average cumulative costs. Shaded regions denote $\pm 1.96 \times$ standard deviations.

Figure 7: Performance of policies on data under distribution shift 1

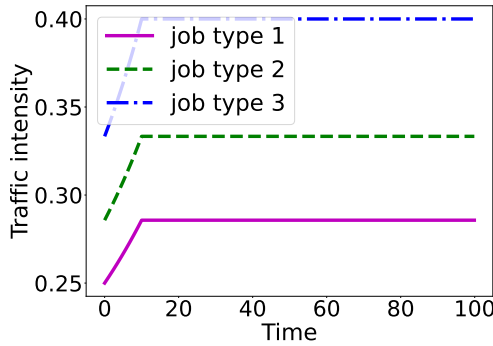


(a) Traffic intensities $\rho(t) = \frac{\lambda(t)}{\mu(t)}$ representing arrival and service rates for each class.

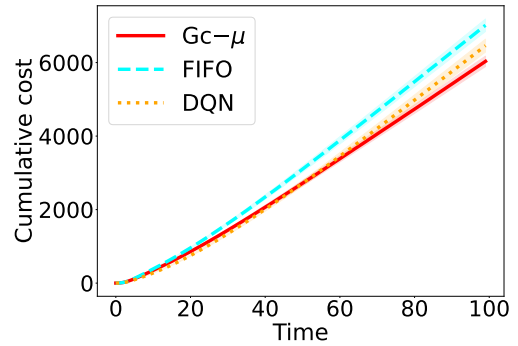


(b) Average cumulative costs. Shaded regions denote $\pm 1.96 \times$ standard deviations.

Figure 8: Performance of policies on data under distribution shift 2

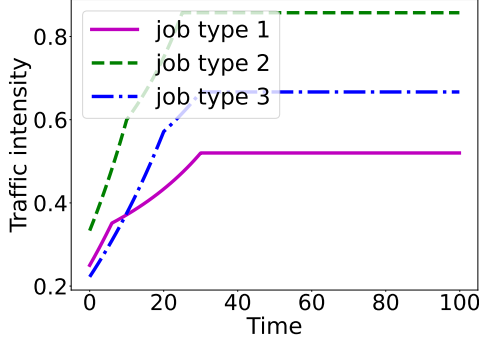


(a) Traffic intensities $\rho(t) = \frac{\lambda(t)}{\mu(t)}$ representing arrival and service rates for each class.

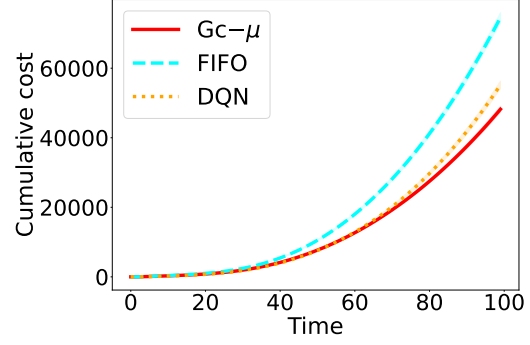


(b) Average cumulative costs. Shaded regions denote $\pm 1.96 \times$ standard deviations.

Figure 9: Performance of policies on data under distribution shift 3

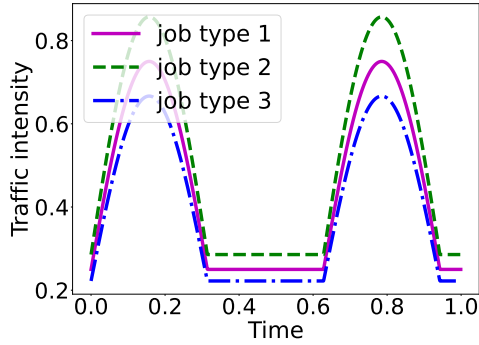


(a) Traffic intensities $\rho(t) = \frac{\lambda(t)}{\mu(t)}$ representing arrival and service rates for each class.

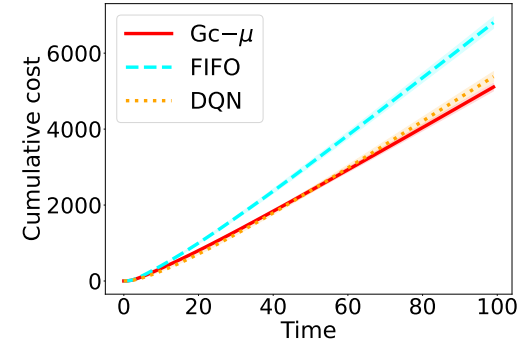


(b) Average cumulative costs. Shaded regions denote $\pm 1.96 \times$ standard deviations.

Figure 10: Performance of policies on data under distribution shift 4



(a) Traffic intensities $\rho(t) = \frac{\lambda(t)}{\mu(t)}$ representing arrival and service rates for each class.



(b) Average cumulative costs. Shaded regions denote $\pm 1.96 \times$ standard deviations.

Figure 11: Performance of policies on data under distribution shift 5

Since we consider cyclical arrival rates in distribution shift 5, we only plot $\rho(t)$ for $t \in [0, 1]$.

To make a fair comparison, we assume that the Gc- μ rule does not know that the underlying system has changed and still uses the (possibly incorrect) original service rate to make decisions. In Figures 7-11, we present performance over 100,000 sample paths on each distribution shift. As suggested by our stability metric, we observe that the simple index-based policy exhibits significant robustness benefits over the engineered DQN approach. Our empirical analysis also shows that the stability metric is no panacea. When the real distribution shift in question is not aligned with the worst-case distribution in the stability measure (1.1), we observe the stability measure may not be so informative in informing performance differentials.

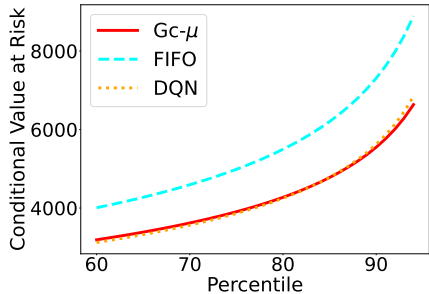


Figure 12. CVaR with quantile level α for different policies

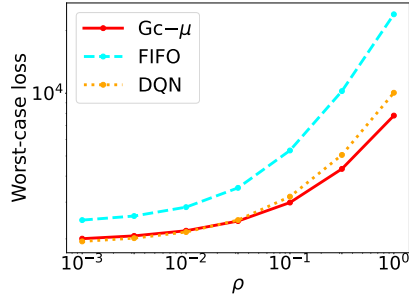


Figure 13. Worst-case expectation over a KL neighborhood of radius ρ for different policies

Finally, we compare our stability measure against other common coherent risk measures. We consider distributionally robust losses—equivalently, coherent risk measures [131, Chapter 6]—over the ambiguity set \mathcal{P}

$$\sup_{Q \in \mathcal{P}} \mathbb{E}_Q[R] \quad \text{where} \quad \mathcal{P}_\rho^{\text{kl}} = \{Q : D_{\text{kl}}(Q \| P) \leq \rho\} \text{ or}$$

$$\mathcal{P}_\alpha^{\text{cvar}} = \{Q : P = aQ + (1-a)Q' \text{ for some probability } Q' \text{ and } 1 \geq a \geq \alpha\}.$$

In particular, $\mathcal{P}_\alpha^{\text{cvar}}$ gives the popular Conditional Value-at-Risk (CVaR) parameterized by the percentile α . As we see in Figure 12, compared to Figure 6, our stability measure is better at differentiating the risk for different policies while CVaR outputs different rankings in risk with different choices of α . Similarly, in Figure 13, we estimate the worst-case expectation under $\mathcal{P}_\rho^{\text{kl}}$ using the dual reformulation (A.4) and we observe that this metric applying on the loss gives different robustness rankings for different choices of ρ .

5.2 Health utilization prediction

As our second example, we analyze a prediction setting where we are interested in whether an individual is utilizing healthcare services based on a rich set of demographic features and medical information. Individual-level predictions can be used to inform a variety of critical operational decisions. Allowing low-income individuals to utilize healthcare resources is a major policy goal [30, 102, 29, 82], and individual-level predictions based on reliable ML models can inform targeted policy-making [85, 8]. Insurance firms can also decide whether or not to enter a new market based on estimates of the new market’s average utilization [148].

Using the National Health Interview Survey (NHIS), we collate a supervised dataset focusing on low-income individuals. We are interested in a binary outcome Y indicating whether the individual visited the doctor’s office in the two weeks before the survey date. We use a rich set of covariates $X \in \mathbb{R}^d$ ($d = 396$) consisting of demographics, earnings, enrollment in government insurance programs (e.g., Medicaid), medical history, and pre-existing conditions. We take the viewpoint of an analyst in 2015 who wishes to train and deploy a prediction model to be used in subsequent years. The NHIS data contains temporal data up to 2018, allowing us to simulate distribution shifts occurring in “future years.” *We use this example to illustrate that stability is a useful complementary measure to the usual average-case prediction evaluations, and highlight the limitations of our approach.*

The distribution of demographic and socioeconomic factors can significantly change over time, leading to large covariate shifts [79]. To illustrate the flexibility of our stability approach, we

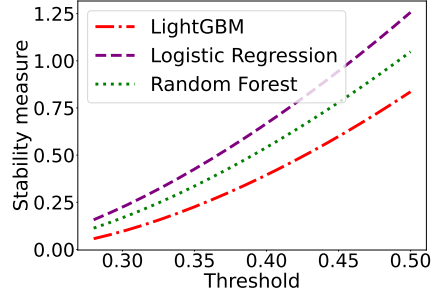


Figure 14: Stability \hat{I}_n for different models over a set of thresholds

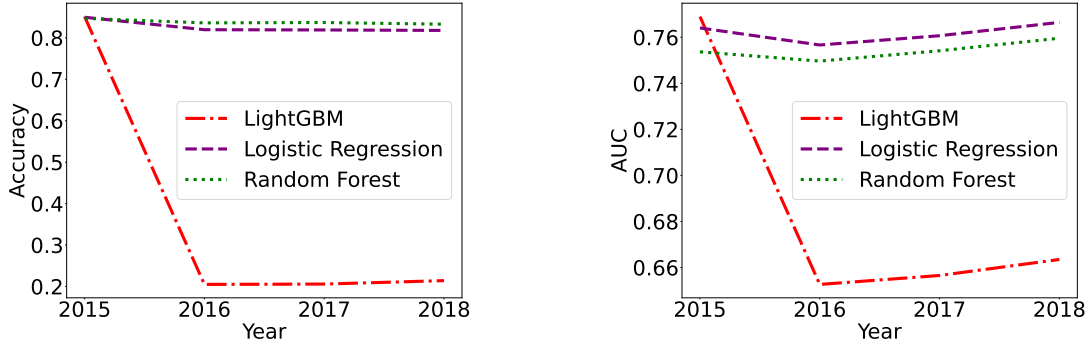
consider a scenario where distribution shift is a major concern only for a subset Z of the covariates X . In contrast to our original framework defined over changes in the joint distribution of (X, Y) , we define the stability measure only over marginal shifts in Z , assuming $(X, Y)|Z$ is fixed. To start, we focus on the following list of core variables: gender, years of education, number of working hours, number of overnight hospital visits, health status, no. home visits by health professionals in the past 2 weeks, whether the main reason for not working last week is due to health, whether the individual received care 10+ times in the past 12 months, months worked last year, limitation regarding all conditions, whether the individual has no coverage of any type, family’s spending on medical care, months without coverage and number of nights in the hospital in the past 12 months, and reported health status. See Table 3 in for a detailed description of these variables.

Formally, let $f(X)$ be a classifier and let $\ell(f(X); Y)$ denote the 0-1 loss. We define our stability measure over the conditional risk

$$R(Z; f) := \mathbb{E}[\ell(f(X); Y)|Z], \quad (5.1)$$

considering shifts in the marginal distribution of Z . Since $R(Z; f)$ is never observed, we estimate it using an *auxiliary* black-box machine learning model for each candidate prediction model $f(\cdot)$ we wish to evaluate. Then, we compute our stability estimator \hat{I}_n based on the approximate data $\{R(Z_i; f)\}_{i=1}^n$. We evaluate the stability of several different prediction modeling frameworks (model classes \mathcal{F}), with a particular focus on tree-based ensemble methods [69] as they provide state-of-the-art performance on tabular data [61]. We train logistic regression and random forest classifiers using the `scikitlearn` package and train a gradient-boosted decision tree using the `LightGBM` package; for all model classes, we use 0.5 as the classification threshold and use standard five-fold cross-validation to select hyperparameters. See Section D.2 for implementation details.

We see that models perform similarly according to average test error: LightGBM: 14.87%, Logistic regression: 15.03%, Random forest: 15.29%. The LightGBM model performs marginally better than the other two models. Going beyond this standard average-case comparison, we evaluate the stability of each model under distribution shift, i.e., assess how much the distribution of $R(Z; f)$ must change until the error rate degrades above the threshold y . For simplicity, we focus on a threshold value y that is approximately thrice the test error of LightGBM; this again unfairly favors the LightGBM model, which has the best average error rate. In a stark reversal compared to the average-case evaluations, we observe that the stability of the LightGBM model is significantly worse than that of the other two models. Indeed, in Figure 14, we observe that LightGBM remains the least stable model for different thresholds. In contrast, if this plot outputs that LightGBM is only stable for certain thresholds, the analyst can document this information, and stakeholders

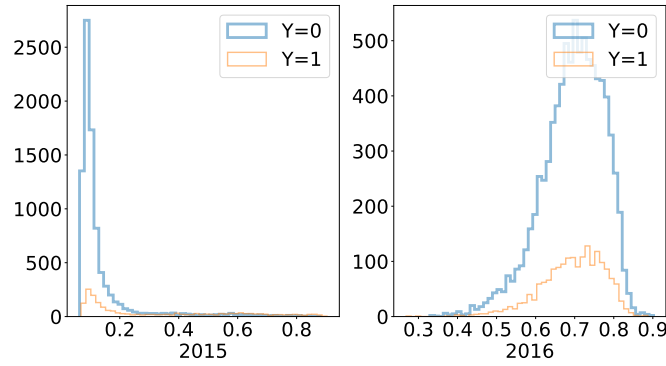


(a) Accuracy across time

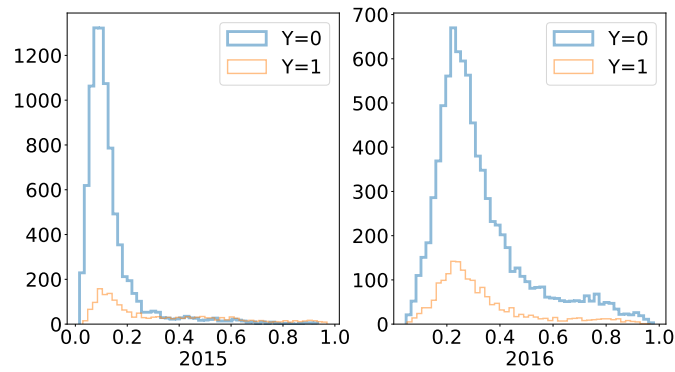
(b) AUC across time

Figure 15: Model performance in “future” years

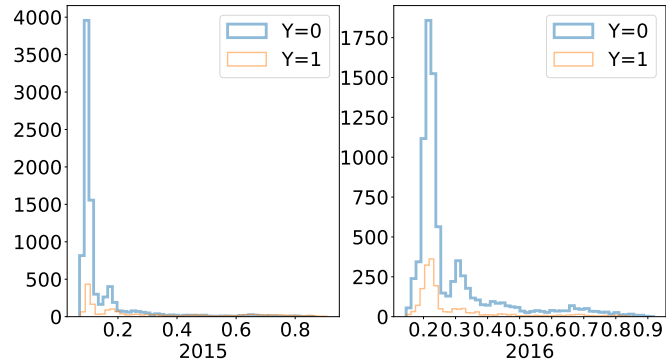
can take it into account for decision-making. Even if the analyst has an exact threshold for model comparison, computing stability around this threshold and making a plot similar to Figure 14 can provide further context. Similar to the queueing example, we compare the stability measure with other risk measures in Section D.2.



(a) LightGBM



(b) Logistic Regression



(c) Random Forest

Figure 16: Histogram of calibrated probabilities for three models across time

To complement our stability evaluations based on worst-case distribution shifts, we evaluate the performance of each prediction model on “future data.” In Figure 15a), we observe that while the performance of the random forest and logistic regression models remain stable, the performance of the LightGBM model substantially degrades over time. The large performance gap is particularly unexpected given near-identical test accuracy on 2015 data. To assess whether the

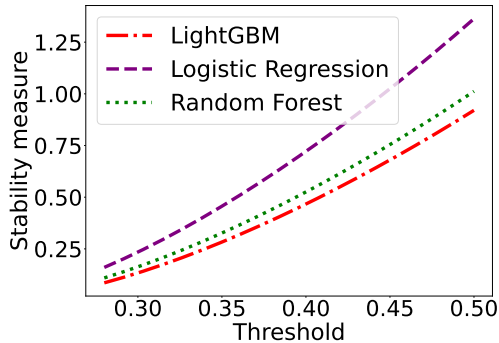


Figure 17: Stability \hat{I}_n for different models over a set of thresholds

issue is simply due to the classification threshold—recall that we had simply set it to 0.5 for all models—we evaluate models using the AUC in Figure 15b) and find similar trends: although adjusting classification thresholds can mitigate instability, the LightGBM model still performs poorly under threshold-invariant AUC evaluations. To understand the severe performance degradation of the LightGBM model, we perform further qualitative analysis. We find that the distribution of (calibrated) classification probabilities changes drastically for the LightGBM model across different years in Figure 16, whereas the shift for the two other models is milder. (We see similar trends persisting across other years.) We observe a large distribution shift in the number of home visits by healthcare professionals over time, which the LightGBM model overly relies on for prediction.

Overall, our stability analysis allows surfacing the flaws of the LightGBM model; it is difficult for the analyst to realize these flaws merely using the average accuracy and AUC on held-out test data from 2015. Our empirical analysis also highlights the limitations of our approach. We carry out the same procedure to compute the stability measure described in Algorithm 2 but with a different set of core variables Z . For concreteness, we focus on the following list of ten core variables: gender, Medicaid enrollment status, years of education, health status, number of working hours, number of overnight hospital visits, number of home visits by healthcare professionals, employment, and retirement status. In Figure 17, we observe that although the stability measure indicates logistic regression is more stable than the random forest classifier, both perform similarly in future years. This suggests that stability measure with these new variables Z may be too conservative for such fine-grained comparisons. A principled selection mechanism for Z is a promising future research topic.

6 Discussion

We study a stability framework for assessing system performance against distribution shifts. Our approach is interpretable as it is parameterized by a level of permissible performance degradation in the cost scale and allows relative comparisons between different system designs as we detail in Section 5. In contrast, a principled choice of the magnitude of distribution shift is a longstanding open problem in the distributional robustness literature; this is often the most important modeling choice that governs subsequent performance evaluations. As humans are typically unable to reason on the scale of distribution shifts, our framework circumvents this problem by considering a dual-like quantity (1.1) defined with respect to the performance threshold y .

Theoretically, the finite sample minimax rates we present in Sections 3 and 4 are one of the first

hardness results in estimating system performance under distribution shifts. Duchi and Namkoong [40], Levy et al. [98] are the only prior works we know of, that showed minimax rates for distributionally robust optimization. Given the connections to large deviations theory delineated in Section 2, we hope the analytic tools developed in this work can spur further formal studies on the statistical estimation of rare event probabilities and large deviation rates [36, 37, 7, 45].

We focus on the formulation (1.1) considering all distribution shifts, but this may often be overly conservative in practice. In many application scenarios, the modeler is concerned with a particular type of distribution shift as discussed in Section 5.2. In prediction, spatial and subpopulation shifts often lead to changes in certain demographic compositions [39, 80, 86]. In causal inference, one is typically concerned with unobserved confounders that impact changes in the distribution of $R | X$, where X is a set of observed covariates [122, 137, 83]. A stability framework over a structured set of distribution shifts—constructed using domain knowledge—is a fruitful future direction.

In many applications, the performance of a system must be evaluated across multiple dimensions. In drug development, both efficacy and potency are crucial. For online platforms, consumer satisfaction and long-term revenue are natural dual objectives. In each case, stability in one dimension may not imply stability in the other. Any robustness evaluation must take into account potential trade-offs, which requires modeling correlation structures. Developing an understanding of stability in such multidimensional settings is an important future research direction.

References

- [1] ACCORD Study Group. Effects of intensive blood-pressure control in type 2 diabetes mellitus. *New England Journal of Medicine*, 362(17):1575–1585, 2010.
- [2] S. M. Ali and S. D. Silvey. A general class of coefficients of divergence of one distribution from another. *Journal of the Royal Statistical Society, Series B*, 28:131–142, 1966.
- [3] E. Amorim, M. Cançado, and A. Veloso. Automated essay scoring in the presence of biased ratings. In *Association for Computational Linguistics (ACL)*, pages 229–237, 2018.
- [4] Anonymous. When robustness doesn’t promote robustness: Synthetic vs. natural distribution shifts on ImageNet. In *Submitted to International Conference on Learning Representations*, 2020. URL <https://openreview.net/forum?id=HyxPIyrFvH>. under review.
- [5] P. Artzner, F. Delbaen, J.-M. Eber, and D. Heath. Coherent measures of risk. *Mathematical Finance*, 9(3):203–228, 1999.
- [6] S. Asmussen. *Ruin probabilities*, volume 2. World scientific, 2000.
- [7] S. Asmussen and P. W. Glynn. *Stochastic Simulation: Algorithms and Analysis*. Springer, 2007.
- [8] S. Athey. Beyond prediction: Using big data for policy problems. *Science*, 355(6324):483–485, 2017.
- [9] F. Bachoc, F. Gamboa, M. Halford, J.-M. Loubes, and L. Risser. Explaining machine learning models using entropic variable projection. *Information and Inference: A Journal of the IMA*, 12(3), 2023.

- [10] P. Bandi, O. Geessink, Q. Manson, M. Van Dijk, M. Balkenhol, M. Hermsen, B. E. Bejnordi, B. Lee, K. Paeng, A. Zhong, et al. From detection of individual metastases to classification of lymph node status at the patient level: the camelyon17 challenge. *IEEE transactions on medical imaging*, 38(2):550–560, 2018.
- [11] A. Banerjee, D. Karlan, and J. Zinman. Six randomized evaluations of microcredit: Introduction and further steps. *American Economic Journal: Applied Economics*, 7(1):1–21, 2015.
- [12] S. Basu, J. B. Sussman, and R. A. Hayward. Detecting heterogeneous treatment effects to guide personalized blood pressure treatment: a modeling study of randomized clinical trials. *Annals of Internal Medicine*, 166(5):354–360, 2017.
- [13] S. Beery, E. Cole, and A. Gjoka. The iwildcam 2020 competition dataset. *arXiv:2004.10340 [cs.CV]*, 2020.
- [14] R. H. Berk. Limiting Behavior of Posterior Distributions when the Model is Incorrect. *The Annals of Mathematical Statistics*, 37(1):51 – 58, 1966.
- [15] J. Blanchet and K. Murthy. Quantifying distributional model risk via optimal transport. *Mathematics of Operations Research*, 44(2):565–600, 2019.
- [16] J. Blanchet, Y. Kang, and K. Murthy. Robust Wasserstein profile inference and applications to machine learning. *Journal of Applied Probability*, 56(3):830–857, 2019.
- [17] J. F. Bonnans and A. Shapiro. *Perturbation Analysis of Optimization Problems*. Springer, 2000.
- [18] G. Brockman, V. Cheung, L. Pettersson, J. Schneider, J. Schulman, J. Tang, and W. Zaremba. OpenAI Gym. *arXiv: 1606.01540 [cs.LG]*, 2016.
- [19] T. Broderick, R. Giordano, and R. Meager. An automatic finite-sample robustness metric: When can dropping a little data make a big difference? *arXiv:2011.14999 [stat.ME]*, 2023.
- [20] L. D. Brown. *Fundamentals of Statistical Exponential Families*. Institute of Mathematical Statistics, Hayward, California, 1986.
- [21] I. Y. Chen, E. Pierson, S. Rose, S. Joshi, K. Ferryman, and M. Ghassemi. Ethical machine learning in health care. *arXiv:2009.10576 [cs.SY]*, 2020.
- [22] M. S. Chen, P. N. Lara, J. H. Dang, D. A. Paterniti, and K. Kelly. Twenty years post-NIH revitalization act: enhancing minority participation in clinical trials (EMPaCT): laying the groundwork for improving minority clinical trial accrual: renewing the case for enhancing minority participation in cancer clinical trials. *Cancer*, 120:1091–1096, 2014.
- [23] I. Cook. Who is driving the great resignation. *Harvard Business Review*, 15, 2021.
- [24] J. Cornfield, W. Haenszel, E. C. Hammond, A. M. Lilienfeld, M. B. Shimkin, and E. L. Wynder. Smoking and lung cancer: Recent evidence and a discussion of some questions. *Journal of the National Cancer Institute*, 22(1):173–203, 1959.
- [25] G. Cruces and S. Galiani. Fertility and female labor supply in latin america: New causal

- evidence. *Labour Economics*, 14(3):565–573, 2007.
- [26] I. Csiszár. Information-type measures of difference of probability distributions and indirect observation. *Studia Scientifica Mathematica Hungaria*, 2:299–318, 1967.
- [27] I. Csiszar. Sanov Property, Generalized I -Projection and a Conditional Limit Theorem. *Annals of Probability*, 12(3):768–793, 1984.
- [28] S. Csorgo and J. L. Teugels. Empirical laplace transform and approximation of compound distributions. *Journal of Applied Probability*, 27(1):88–101, 1990.
- [29] J. Currie and J. Fahr. Medicaid managed care: effects on children’s medicaid coverage and utilization. *Journal of Public Economics*, 89(1):85–108, 2005.
- [30] J. Currie and J. Gruber. Health insurance eligibility, utilization of medical care, and child health. *The Quarterly Journal of Economics*, 111(2):431–466, 1996.
- [31] J. G. Dai and M. Gluzman. Queueing network controls via deep reinforcement learning. *Stochastic Systems*, pages 1–38, 2021.
- [32] A. D’Amour, K. Heller, D. Moldovan, B. Adlam, B. Alipanahi, A. Beutel, C. Chen, J. Deaton, J. Eisenstein, M. D. Hoffman, et al. Underspecification presents challenges for credibility in modern machine learning. *Journal of Machine Learning Research*, 23(226):1–61, 2022.
- [33] L. De Haan and A. Ferreira. *Extreme Value Theory: An Introduction*. Springer Science & Business Media, 2007.
- [34] R. Dehejia, C. Pop-Eleches, and C. Samii. From local to global: External validity in a fertility natural experiment. *Journal of Business & Economic Statistics*, 39(1):217–243, 2021.
- [35] F. Delbaen. Coherent risk measures on general probability spaces. In *Advances in finance and stochastics*, pages 1–37. Springer, 2002.
- [36] A. Dembo and O. Zeitouni. *Large Deviations Techniques and Applications*. Springer-Verlag, 1998.
- [37] J.-D. Deuschel and D. W. Stroock. *Large deviations*, volume 137. Academic press Boston, 1989.
- [38] M. D. Donsker and S. R. S. Varadhan. Asymptotic evaluation of certain Markov process expectations for large time-iii. *Communications on Pure and Applied Mathematics*, 29(4):389–461, 1976.
- [39] J. Duchi, T. Hashimoto, and H. Namkoong. Distributionally robust losses for latent covariate mixtures. *Operations Research*, 2022.
- [40] J. C. Duchi and H. Namkoong. Learning models with uniform performance via distributionally robust optimization. *Annals of Statistics*, 49(3):1378–1406, 2021.
- [41] J. C. Duchi, P. W. Glynn, and H. Namkoong. Statistics of robust optimization: A generalized empirical likelihood approach. *Mathematics of Operations Research*, 46:946–969, 2021.
- [42] K. Duffy and A. P. Metcalfe. The large deviations of estimating rate functions. *Journal of*

- Applied Probability*, 42(1):267–274, 2005.
- [43] K. R. Duffy and B. D. Williamson. Estimating large deviation rate functions. *arXiv:1511.02295 [math.PR]*, 2015.
- [44] S. G. Eick, W. A. Massey, and W. Whitt. $M_t/G/\infty$ queues with sinusoidal arrival rates. *Management Science*, 39(2):241–252, 1993.
- [45] R. Ellis. *Entropy, large deviations, and statistical mechanics*. Springer, 2007.
- [46] W. Feller. *An introduction to probability theory and its applications*, volume 2. John Wiley & Sons, 1971.
- [47] A. Feuerverger. On the empirical saddlepoint approximation. *Biometrika*, 76(3):457–464, 1989.
- [48] A. Feuerverger and R. A. Mureika. The empirical characteristic function and its applications. *Annals of Statistics*, pages 88–97, 1977.
- [49] D. Freund and S. B. Hopkins. Towards practical robustness auditing for linear regression. *arXiv:2307.16315 [stat.ME]*, 2023.
- [50] R. Gao and A. J. Kleywegt. Distributionally robust stochastic optimization with Wasserstein distance. *Mathematics of Operations Research*, 2022.
- [51] N. Garg and H. Nazerzadeh. Driver surge pricing. *Management Science*, 68(5):3219–3235, 2022.
- [52] P. Gertler, M. Shah, M. L. Alzua, L. Cameron, S. Martinez, and S. Patil. How does health promotion work? evidence from the dirty business of eliminating open defecation. Technical report, National Bureau of Economic Research, 2015.
- [53] S. Ghosh and H. Lam. Robust analysis in stochastic simulation: Computation and performance guarantees. *Operations Research*, 2019.
- [54] P. Glasserman. *Monte Carlo methods in financial engineering*, volume 53. Springer, 2004.
- [55] P. Glasserman and X. Xu. Robust risk measurement and model risk. *Quantitative Finance*, 14(1):29–58, 2013.
- [56] P. Glasserman and L. Yang. Bounding wrong-way risk in CVA calculation. *Mathematical Finance*, 28(1):268–305, 2018.
- [57] P. W. Glynn and Z. Zheng. Estimation and inference for non-stationary arrival models with a linear trend. In *Winter Simulation Conference (WSC)*, pages 3764–3773. IEEE, 2019.
- [58] A. Goeva, H. Lam, H. Qian, and B. Zhang. Optimization-based calibration of simulation input models. *Operations research*, page 1362–1382, 2019.
- [59] L. Green and P. Kolesar. Testing the validity of a queueing model of police patrol. *Management Science*, 35(2):127–148, 1989.
- [60] L. Green, P. Kolesar, and A. Svoronos. Some effects of nonstationarity on multiserver Marko-

- vian queueing systems. *Operations Research*, 39(3):502–511, 1991.
- [61] L. Grinsztajn, E. Oyallon, and G. Varoquaux. Why do tree-based models still outperform deep learning on tabular data? In *Thirty-sixth Conference on Neural Information Processing Systems Datasets and Benchmarks Track*, 2022.
- [62] S. Gu, E. Holly, T. Lillicrap, and S. Levine. Deep reinforcement learning for robotic manipulation with asynchronous off-policy updates. In *International Conference on Robotics and Automation*, pages 3389–3396. IEEE, 2017.
- [63] S. Gupta and D. Rothenhäusler. The s -value: evaluating stability with respect to distributional shifts. *arXiv: 2105.03067 [stat.ME]*, 2021.
- [64] P. Hall, J. L. Teugels, and A. Vanmarcke. The abscissa of convergence of the Laplace transform. *Journal of Applied Probability*, pages 353–362, 1992.
- [65] D. J. Hand. Classifier technology and the illusion of progress. *Statistical Science*, 21(1):1–14, 2006.
- [66] L. P. Hansen and T. J. Sargent. Robust control and model uncertainty. *American Economic Review*, 91(2):60–66, 2001.
- [67] J. M. Harrison and L. M. Wein. Scheduling networks of queues: Heavy traffic analysis of a simple open network. *Queueing Systems*, pages 265–280, 1989.
- [68] J. M. Harrison and A. Zeevi. Dynamic scheduling of a multiclass queue in the halfin-whitt heavy traffic regime. *Operations Research*, 52(2):243–257, 2004.
- [69] T. Hastie, R. Tibshirani, and J. Friedman. *The Elements of Statistical Learning*. Springer, second edition, 2009.
- [70] M. J. Hausknecht and P. Stone. Deep recurrent Q-learning for partially observable MDPs. In *Proceedings of the Thirty-Second National Conference on Artificial Intelligence*, 2015.
- [71] K. He, X. Zhang, S. Ren, and J. Sun. Delving deep into rectifiers: Surpassing human-level performance on imagenet classification. In *Proceedings of the International Conference on Computer Vision*, pages 1026–1034, 2015.
- [72] P. Henderson, R. Islam, P. Bachman, J. Pineau, D. Precup, and D. Meger. Deep reinforcement learning that matters. In *Thirty-Second AAAI Conference on Artificial Intelligence*. AAAI Press, 2018.
- [73] T. Homma and A. Saltelli. Importance measures in global sensitivity analysis of nonlinear models. *Reliability Engineering & System Safety*, 52(1):1–17, 1996.
- [74] Y. Hu, C. W. Chan, and J. Dong. Prediction-driven surge planning with application in the emergency department. *Preprint*, 2021.
- [75] Z. Hu and J. Hong. Kullback-Leibler divergence constrained distributionally robust optimization. *Available at Optimization Online*, 2013.
- [76] P. J. Huber. *Robust Statistics*. John Wiley and Sons, New York, 1981.

- [77] P. J. Huber and E. M. Ronchetti. *Robust Statistics*. John Wiley and Sons, second edition, 2009.
- [78] J. P. Ioannidis. Why most published research findings are false. *PLoS Medicine*, 2(8), 2005. doi: 10.1371/journal.pmed.0020124.
- [79] S. Jeong and H. Namkoong. Robust causal inference under covariate shift via worst-case subpopulation treatment effect. In *Proceedings of the Thirty Third Annual Conference on Computational Learning Theory*, 2020.
- [80] S. Jeong and H. Namkoong. Assessing external validity over worst-case subpopulations. *arXiv:2007.02411 [stat.ML]*, 2020.
- [81] W. X. Jiang, B. L. Nelson, and L. J. Hong. Estimating sensitivity to input model variance. In *Proceedings of the Winter Simulation Conference*, page 3705–3716, 2019.
- [82] J. Kahende, A. Malarcher, L. England, L. Zhang, P. Mowery, X. Xu, V. Sevilimedu, and I. Rolle. Utilization of smoking cessation medication benefits among medicaid fee-for-service enrollees 1999–2008. *Public Library of Science One*, 12(2):e0170381, 2017.
- [83] N. Kallus and A. Zhou. Confounding-robust policy improvement. In *Advances in Neural Information Processing Systems 31*, pages 9269–9279, 2018.
- [84] D. P. Kingma and J. Ba. Adam: A method for stochastic optimization. In *Proceedings of the Third International Conference on Learning Representations*, 2015.
- [85] J. Kleinberg, J. Ludwig, S. Mullainathan, and Z. Obermeyer. Prediction policy problems. *American Economic Review*, 105(5):491–95, 2015.
- [86] P. W. Koh, S. Sagawa, H. Marklund, S. M. Xie, M. Zhang, A. Balsubramani, W. Hu, M. Yasunaga, R. L. Phillips, S. Beery, et al. Wilds: A benchmark of in-the-wild distribution shifts. *arXiv:2012.07421 [cs.LG]*, 2020.
- [87] B. O. Koopman. Air-terminal queues under time-dependent conditions. *Operations Research*, 20(6):1089–1114, 1972.
- [88] D. Kuhn, P. M. Esfahani, V. A. Nguyen, and S. Shafieezadeh-Abadeh. Wasserstein distributionally robust optimization: Theory and applications in machine learning. In *Operations Research & Management Science in the Age of Analytics*, pages 130–166. INFORMS, 2019.
- [89] H. Lam. Robust sensitivity analysis for stochastic systems. *Mathematics of Operations Research*, 41(4):1248–1275, 2016.
- [90] H. Lam. Advanced tutorial: Input uncertainty and robust analysis in stochastic simulation. In *Proceedings of the 2016 Winter Simulation Conference*, page 178–192, 2016.
- [91] H. Lam. Sensitivity to serial dependency of input processes: A robust approach. *Management Science*, 64(3):1311–1327, 2017.
- [92] H. Lam and H. Qian. Optimization-based quantification of simulation input uncertainty via empirical likelihood. *arXiv:1707.05917 [stat.ME]*, 2019.

- [93] H. Lam and E. Zhou. The empirical likelihood approach to quantifying uncertainty in sample average approximation. *Operations Research Letters*, 45(4):301–307, 2017.
- [94] L. Le Cam. Convergence of estimates under dimensionality restrictions. *Annals of Statistics*, 1(1):38–53, 1973.
- [95] L. Le Cam. *Asymptotic Methods in Statistical Decision Theory*. Springer-Verlag, 1986.
- [96] J. T. Leek, R. B. Scharpf, H. C. Bravo, D. Simcha, B. Langmead, W. E. Johnson, D. Geman, K. Baggerly, and R. A. Irizarry. Tackling the widespread and critical impact of batch effects in high-throughput data. *Nature Reviews Genetics*, 11(10):733–739, 2010.
- [97] P. Lemaître, E. Sergienko, A. Arnaud, N. Bousquet, F. Gamboa, and B. Iooss. Density modification-based reliability sensitivity analysis. *Journal of Statistical Computation and Simulation*, 85(6):1200–1223, 2015.
- [98] D. Levy, Y. Carmon, J. C. Duchi, and A. Sidford. Large-scale methods for distributionally robust optimization. In *Advances in Neural Information Processing Systems 33*, 2020.
- [99] M. Li, H. Namkoong, and S. Xia. Evaluating model performance under worst-case subpopulations. In *Advances in Neural Information Processing Systems 34*, volume 34, 2021.
- [100] Q. Li, J. B. Brown, H. Huang, and P. J. Bickel. Measuring reproducibility of high-throughput experiments. *The Annals of Applied Statistics*, 5(3):1752 – 1779, 2011.
- [101] L. J. Lin. Self-improving reactive agents based on reinforcement learning, planning, and teaching. *Machine Learning*, 8:293–321, 1992.
- [102] B. J. Lipton and S. L. Decker. The effect of health insurance coverage on medical care utilization and health outcomes: Evidence from medicaid adult vision benefits. *Journal of health economics*, 44:320–332, 2015.
- [103] B. Liu, Q. Xie, and E. Modiano. Reinforcement learning for optimal control of queueing systems. In *2019 57th Annual Allerton Conference on Communication, Control, and Computing (Allerton)*, pages 663–670, 2019.
- [104] D. Z. Long, M. Sim, and M. Zhou. Robust satisficing. *Operations Research*, 71(1):61–82, 2023.
- [105] D. Luenberger. *Optimization by Vector Space Methods*. Wiley, 1969.
- [106] A. Mandelbaum and A. L. Stolyar. Scheduling flexible servers with convex delay costs: Heavy-traffic optimality of the generalized $c\mu$ -rule. *Operations Research*, 52(6):836–855, 2004.
- [107] C. F. Manski. *Public policy in an uncertain world*. Harvard University Press, 2013.
- [108] R. Maronna, D. Martin, and V. Yohai. *Robust Statistics: Theory and Methods*. Wiley Series in Probability and Statistics. Wiley, 2006.
- [109] V. Mnih, K. Kavukcuoglu, D. Silver, A. Graves, I. Antonoglou, D. Wierstra, and M. Riedmiller. Playing Atari with deep reinforcement learning. *arXiv:1312.5602 [cs.LG]*, 2013.
- [110] A. Moitra and D. Rohatgi. Provably auditing ordinary least squares in low dimensions. In

- Proceedings of the Eleventh International Conference on Learning Representations*, 2023.
- [111] W. J. Murdoch, C. Singh, K. Kumbier, R. Abbasi-Asl, and B. Yu. Definitions, methods, and applications in interpretable machine learning. *Proceedings of the National Academy of Sciences*, 116(44):22071–22080, 2019.
- [112] A. Niculescu-Mizil and R. Caruana. Predicting good probabilities with supervised learning. In *Proceedings of the 22nd International Conference on Machine Learning*, page 625–632, 2005.
- [113] A. B. Owen. Sobol’ indices and Shapley value. *SIAM/ASA Journal on Uncertainty Quantification*, 2(1):245–251, 2014.
- [114] C. H. Papadimitriou and J. N. Tsitsiklis. The complexity of optimal queueing network control. *Mathematics of Operations Research*, 24(2):293–305, 1999.
- [115] A. Paszke, S. Gross, F. Massa, A. Lerer, J. Bradbury, G. Chanan, T. Killeen, Z. Lin, N. Gimelshein, L. Antiga, A. Desmaison, A. Kopf, E. Yang, Z. DeVito, M. Raison, A. Tejani, S. Chilamkurthy, B. Steiner, L. Fang, J. Bai, and S. Chintala. PyTorch: An imperative style, high-performance deep learning library. In *Advances in Neural Information Processing Systems 19*, volume 32, 2019.
- [116] H. Rahimian and S. Mehrotra. Distributionally robust optimization: A review. *arXiv:1908.05659 [math.OC]*, 2019.
- [117] R. T. Rockafellar. *Convex Analysis*. Princeton University Press, 1970.
- [118] R. T. Rockafellar. Coherent approaches to risk in optimization under uncertainty. *Tutorials in Operations Research*, 3:38–61, 2007.
- [119] R. T. Rockafellar and S. Uryasev. Optimization of conditional value-at-risk. *Journal of Risk*, 2:21–42, 2000.
- [120] R. T. Rockafellar, S. Uryasev, and M. Zabarankin. Generalized deviations in risk analysis. *Finance and Stochastics*, 10(1):51–74, 2006.
- [121] C. M. Rohwer, F. Angeletti, and H. Touchette. Convergence of large-deviation estimators. *Physical Review E*, 92(5):052104, 2015.
- [122] P. R. Rosenbaum. Observational studies. In *Observational studies*, pages 1–17. Springer, 2002.
- [123] P. R. Rosenbaum. *Design of Observational Studies*. Springer Series in Statistics. Springer, 2010.
- [124] P. R. Rosenbaum. A new u-statistic with superior design sensitivity in matched observational studies. *Biometrics*, 67(3):1017–1027, 2011.
- [125] M. R. Rosenzweig and C. Udry. External validity in a stochastic world: Evidence from low-income countries. *Review of Economic Studies*, 87(1):343–381, 2020.
- [126] S. Ross. *Stochastic processes*. Wiley series in probability and statistics: Probability and

- statistics. Wiley, 1996.
- [127] A. Ruszczyński and A. Shapiro. Optimization of convex risk functions. *Mathematics of Operations Research*, 31(3):433–452, 2006.
 - [128] K. Saenko, B. Kulis, M. Fritz, and T. Darrell. Adapting visual category models to new domains. In *Proceedings of the European Conference on Computer Vision*, pages 213–226. Springer, 2010.
 - [129] A. Saltelli, M. Ratto, T. Andres, F. Campolongo, J. Cariboni, D. Gatelli, M. Saisana, and S. Tarantola. *Global sensitivity analysis: the primer*. John Wiley & Sons, 2008.
 - [130] A. Shapiro. Distributionally robust stochastic programming. *SIAM Journal on Optimization*, 27(4):2258–2275, 2017.
 - [131] A. Shapiro, D. Dentcheva, and A. Ruszczyński. *Lectures on Stochastic Programming: Modeling and Theory*. SIAM and Mathematical Programming Society, 2009.
 - [132] D. Silver, J. Schrittwieser, K. Simonyan, I. Antonoglou, A. Huang, A. Guez, T. Hubert, L. Baker, M. Lai, and A. Bolton. Mastering the game of Go without human knowledge. *Nature*, 550(7676):354, 2017.
 - [133] E. Song, B. L. Nelson, and C. D. Pegden. Advanced tutorial: Input uncertainty quantification. In *Proceedings of the Winter Simulation Conference 2014*, pages 162–176, 2014.
 - [134] E. Song, B. L. Nelson, and J. Staum. Shapley effects for global sensitivity analysis: Theory and computation. *SIAM/ASA Journal on Uncertainty Quantification*, 4(1):1060–1083, 2016.
 - [135] SPRINT Research Group. A randomized trial of intensive versus standard blood-pressure control. *New England Journal of Medicine*, 373(22):2103–2116, 2015.
 - [136] V. Stodden. Reproducing statistical results. *Annual Review of Statistics and Its Application*, 2(1):1–19, 2015.
 - [137] Z. Tan. A distributional approach for causal inference using propensity scores. *Journal of the American Statistical Association*, 101(476):1619–1637, 2006.
 - [138] E. Tipton and R. B. Olsen. A review of statistical methods for generalizing from evaluations of educational interventions. *Educational Researcher*, 47(8):516–524, 2018.
 - [139] E. Tipton and L. R. Peck. A design-based approach to improve external validity in welfare policy evaluations. *Evaluation review*, 41(4):326–356, 2017.
 - [140] H. Touchette. The large deviation approach to statistical mechanics. *Physics Reports*, 478(1):1–69, 2009.
 - [141] A. B. Tsybakov. *Introduction to Nonparametric Estimation*. Springer, 2009.
 - [142] A. W. van der Vaart and J. A. Wellner. *Weak Convergence and Empirical Processes: With Applications to Statistics*. Springer, New York, 1996.
 - [143] J. A. Van Mieghem. Dynamic scheduling with convex delay costs: The generalized c - μ rule. *Annals of Applied Probability*, pages 809–833, 1995.

- [144] B. P. Van Parys, P. M. Esfahani, and D. Kuhn. From data to decisions: Distributionally robust optimization is optimal. *Management Science*, 67(6):3387–3402, 2021.
- [145] M. J. Wainwright. *High-Dimensional Statistics: A Non-Asymptotic Viewpoint*. Cambridge University Press, 2019.
- [146] N. Walton and K. Xu. Learning and information in stochastic networks and queues. In *Tutorials in Operations Research: Emerging Optimization Methods and Modeling Techniques with Applications*, pages 161–198. INFORMS, 2021.
- [147] L. Wasserman. *All of nonparametric statistics*. Springer Science & Business Media, 2006.
- [148] D. Wei, K. N. Ramamurthy, and K. R. Varshney. Health insurance market risk assessment: Covariate shift and k -anonymity. In *SIAM International Conference on Data Mining*, 2015.
- [149] A. Weiss and A. Shwartz. *Large deviations for performance analysis*. Chapman and Hall, Boca Raton, 1995.
- [150] W. Whitt. *Stochastic Process Limits: An Introduction to Stochastic Process Limits and Their Application to Queues*. Springer Science & Business Media, 2002.
- [151] R. A. Wijsman. A useful inequality on ratios of integrals, with application to maximum likelihood estimation. *Journal of the American Statistical Association*, 80(390):472–475, 1985.
- [152] R. J. Williams. Stochastic processing networks. *Annual Review of Statistics and Its Application*, 3(1):323–345, 2016.
- [153] A. Wong, E. Otles, J. P. Donnelly, A. Krumm, J. McCullough, O. DeTroyer-Cooley, J. Pestrue, M. Phillips, J. Konye, C. Penozza, et al. External validation of a widely implemented proprietary sepsis prediction model in hospitalized patients. *JAMA Internal Medicine*, 181(8):1065–1070, 2021.
- [154] S. Yadlowsky, H. Namkoong, S. Basu, J. Duchi, and L. Tian. Bounds on the conditional and average treatment effect with unobserved confounding factors. *Annals of Statistics*, 50(5):2587–2615, 2022.
- [155] B. Yu. Assouad, Fano, and Le Cam. In *Festschrift for Lucien Le Cam*, pages 423–435. Springer-Verlag, 1997.
- [156] B. Yu. Stability. *Bernoulli*, 19(4):1484 – 1500, 2013.
- [157] J. R. Zech, M. A. Badgeley, M. Liu, A. B. Costa, J. J. Titano, and E. K. Oermann. Variable generalization performance of a deep learning model to detect pneumonia in chest radiographs: a cross-sectional study. *PLoS medicine*, 15(11):e1002683, 2018.
- [158] L. Zhang, J. Yang, and R. Gao. A simple and general duality proof for Wasserstein distributionally robust optimization. *arXiv:2205.00362 [math.OA]*, 2022.

A Duality results

A.1 Proof of Lemma 1

Since $y \geq \mathbb{E}_P[R]$, we have $\lambda^* \geq 0$ by Jensen's inequality. To prove the first result of the lemma, it suffices to show that

$$I_y(P) = \sup_{\lambda \geq 0} \left\{ \lambda y - \log \mathbb{E}_P[e^{\lambda R}] \right\}.$$

Consider the likelihood ratio formulation (2.1). Introducing Lagrange multipliers $\lambda \geq 0$ for the constraint $\mathbb{E}_P[LR] \geq y$ and η for the constraint $\mathbb{E}_P[L] = 1$, the Lagrangian is given by

$$\mathcal{L}(L, \lambda, \eta) := \mathbb{E}_P[L \log L] - \lambda(\mathbb{E}_P[LR] - y) - \eta(\mathbb{E}_P[L] - 1).$$

Taking $L(R) = \frac{e^{\mu R}}{\mathbb{E}_P[e^{\mu R}]}$ for μ large enough so that $\mathbb{E}_P[LR] > y$, extended Slater's condition holds. Standard functional duality theory (e.g., Luenberger [105, Theorem 8.6.1, Problem 8.7], Bonnans and Shapiro [17, Theorem 2.165]) shows that there is no duality gap. We hence arrive at

$$\begin{aligned} & \inf_{L \geq 0} \{ \mathbb{E}_P[L \log L] : \mathbb{E}_P[LR] \geq y, \mathbb{E}_P[L] = 1 \} \\ &= \sup_{\lambda \geq 0, \eta \in \mathbb{R}} \inf_{L \geq 0} \{ \mathbb{E}_P[L \log L] - \lambda(\mathbb{E}_P[LR] - y) - \eta(\mathbb{E}_P[L] - 1) \}, \end{aligned}$$

where the infimums are taken over measurable functions.

We wish to interchange the inner infimum and the integral. For any fixed $\lambda \geq 0$ and $\eta \in \mathbb{R}$,

$$\begin{aligned} & \inf_{L \geq 0} \{ \mathbb{E}_P[L \log L] - \lambda(\mathbb{E}_P[LR] - y) - \eta(\mathbb{E}_P[L] - 1) \} \\ & \geq \mathbb{E}_P \left[\inf_{l \geq 0} \{ l \log l - \lambda R l - \eta l \} \right] + \lambda y + \eta. \end{aligned} \tag{A.1}$$

Using the first-order optimality condition for the infimum over $l \geq 0$, we see that the minimum is obtained at

$$l^* = \exp(\lambda R + \eta - 1). \tag{A.2}$$

Since $L^* := \exp(\lambda R + \eta - 1)$ is clearly measurable, we conclude equality holds in place of the inequality (A.1).

Plugging the optimal solution (A.2) in the problem (A.1), the dual simplifies to

$$\sup_{\lambda \geq 0, \eta \in \mathbb{R}} \left\{ \lambda y + \eta - e^{\eta-1} \mathbb{E}_P \left[e^{\lambda R} \right] \right\}.$$

Noting that we can restrict attention to λ such that $\mathbb{E}_P[e^{\lambda R}] < \infty$, directly supremizing over η gives $\eta^* = 1 - \log \mathbb{E}_P[e^{\lambda R}]$, which yields the first result. The second result follows from strong duality and the characterization (A.2).

A.2 Duality results for other metrics

We first extend the duality result to f -divergence. Let $f : \mathbb{R} \rightarrow \mathbb{R}_+ \cup \{\infty\}$ be a convex function satisfying $f(1) = 0$ and $f(t) = \infty$ for any $t < 0$. We define the f -divergence [2, 26] between Q and P as

$$D_f(Q \| P) := \int f \left(\frac{dQ}{dP} \right) dP.$$

The f -divergence is quite general and it covers the following commonly used metrics:

1. KL divergence: $f(x) = x \log x - x + 1$
2. Total variation: $f(x) = \frac{1}{2}|x - 1|$
3. χ^2 -divergence: $f(x) = (x - 1)^2$

We refer the reader to [116, Table 1] for more examples of divergence metrics.

The following proposition extends the duality result for KL divergence through the Fenchel conjugate.

Proposition 1. *Let f^* be the Fenchel conjugate of f : $f^*(s) := \sup_t \{st - f(t)\}$. For every y with $\mathbb{E}_P[R] \leq y < \text{ess sup } R$,*

$$\inf_Q \{D_f(Q\|P) : \mathbb{E}_Q[R] \geq y\} = \sup_{\lambda \geq 0, \eta \in \mathbb{R}} \{\lambda y + \eta - \mathbb{E}_P[f^*(\lambda R + \eta)]\}.$$

Proof Similar to (2.1), we have

$$\inf_Q \{D_f(Q\|P) : \mathbb{E}_Q[R] \geq y\} = \inf_{L \geq 0} \{\mathbb{E}_P[f(L)] : \mathbb{E}_P[LR] \geq y, \mathbb{E}_P[L] = 1\},$$

We follow the same proof as in Lemma 1 but replace $L \log L$ with $f(L)$ and $l \log l$ with $f(l)$. Now, (A.1) changes to

$$\lambda y + \eta - \mathbb{E}_P[f^*(\lambda R + \eta)],$$

the rest is similar and we complete the proof. \square

We can also extend Lemma 1 to Wasserstein distances. Let $R \in \mathcal{X}$, where \mathcal{X} is a Polish space, and $\mathcal{P}(\mathcal{X})$ denote all probability distributions. The Wasserstein distance induced by the cost function c is

$$W_c(Q, P) := \inf_{\pi \in \Pi(P, Q)} \left\{ \mathbb{E}_{(R, \hat{R}) \sim \pi} [c(R, \hat{R})] \right\}, \quad Q, P \in \mathcal{P}(\mathcal{X}),$$

where $\Pi(P, Q)$ is the set of probability distributions on $\mathcal{X} \times \mathcal{X}$ with marginals P and Q . Throughout, we impose the following assumption on the cost function c , which is standard in the literature [15].

Assumption A. *The function $c : \mathcal{X} \times \mathcal{X} \rightarrow [0, \infty)$ is lower semicontinuous and $c(x, x) = 0$ for every $x \in \mathcal{X}$.*

We first state a useful technical result.

Lemma 2. [158, Proposition 1, Lemma 2, and Example 2] *Consider any measurable function $\phi : \mathcal{X} \times \mathcal{X} \rightarrow \mathbb{R} \cup \{-\infty\}$. Then*

$$\mathbb{E}_{R \sim P} \left[\sup_{x \in \mathcal{X}} \phi(R, x) \right] = \sup_{\pi \in \Pi_P} \left\{ \mathbb{E}_{(R, \hat{R}) \sim \pi} [\phi(R, \hat{R})] \right\},$$

where Π_P is set of probability distributions π on $\mathcal{X} \times \mathcal{X}$ whose first marginal is P such that $\mathbb{E}_{(R, \hat{R}) \sim \pi} [\phi(R, \hat{R})]$ is well-defined.

To compute the stability measure defined using the Wasserstein distance, we present the following result, which reformulates an infinite-dimensional problem to a low-dimensional problem involving computing the term ψ_λ .

Proposition 2. *Assume assumption A holds. Then*

$$\inf_Q \{W_c(Q, P) : \mathbb{E}_Q[R] \geq y\} = \sup_{\lambda \geq 0} \{\lambda y - \mathbb{E}_P[\psi_\lambda(R)]\},$$

where

$$\psi_\lambda(z) = \sup_{x \in \mathcal{X}} \{\lambda x - c(z, x)\}.$$

Proof We use a proof inspired by Zhang et al. [158]. Fix P , let $L(y) = \inf_Q \{W_c(Q, P) : \mathbb{E}_Q[R] \geq y\}$, and define

$$G(\lambda) = \inf_{y \in \mathbb{R}} \{L(y) - \lambda y\} = -L^*(\lambda),$$

where L^* is the Fenchel conjugate of L . Note that $G(\lambda) = -\infty$ for any $\lambda < 0$. We start by showing that $L(\cdot)$ is a convex function. To see this, we fix $\alpha \in [0, 1]$ and let $\mathcal{Q}_y := \{Q : \mathbb{E}_Q[R] \geq y\}$ for any y and take $Q_x \in \mathcal{Q}_x, Q_y \in \mathcal{Q}_y$. Fix x, y and let $z = \alpha x + (1 - \alpha)y$. Then, letting $Q^* = \alpha Q_x + (1 - \alpha)Q_y$, we have $\mathbb{E}_{Q^*}[R] = \alpha \mathbb{E}_{Q_x}[R] + (1 - \alpha) \mathbb{E}_{Q_y}[R] \geq \alpha x + (1 - \alpha)y = z$ so that $Q^* \in \mathcal{Q}_z$. In addition,

$$L(z) \leq W_c(Q^*, P) \leq \alpha W_c(Q_x, P) + (1 - \alpha)W_c(Q_y, P),$$

taking infimum over $Q_x \in \mathcal{Q}_x$ and $Q_y \in \mathcal{Q}_y$, we arrive at

$$L(z) \leq \alpha L(x) + (1 - \alpha)L(y),$$

and therefore $L(\cdot)$ is convex. Standard arguments from convex analysis [117, Theorem 12.2] imply that

$$L(y) = \sup_{\lambda \in \mathbb{R}} \{\lambda y + G(\lambda)\} = \sup_{\lambda \geq 0} \{\lambda y + G(\lambda)\}, \quad (\text{A.3})$$

where the second equality follows from the fact that $G(\lambda) = -\infty$ for any $\lambda < 0$.

Next, for any $\lambda \geq 0$,

$$\begin{aligned} G(\lambda) &= \inf_{y \in \mathbb{R}} \left\{ \inf_Q \{W_c(Q, P) : \mathbb{E}_Q[R] \geq y\} - \lambda y \right\} \\ &= \inf_{y \in \mathbb{R}} \left\{ \inf_Q \{W_c(Q, P) - \lambda y : \mathbb{E}_Q[R] \geq y\} \right\} \\ &= \inf_Q \left\{ \inf_{y \in \mathbb{R}} \{W_c(Q, P) - \lambda y : \mathbb{E}_Q[R] \geq y\} \right\} \\ &= \inf_Q \{W_c(Q, P) - \lambda \mathbb{E}_Q[R]\}. \end{aligned}$$

Using the definition

$$W_c(Q, P) = \inf_{\pi \in \Pi(P, Q)} \mathbb{E}_{(R, \hat{R}) \sim \pi} [c(R, \hat{R})],$$

we have

$$G(\lambda) = \inf_Q \left\{ \inf_{\pi \in \Pi(P, Q)} \mathbb{E}_{(R, \hat{R}) \sim \pi} [c(R, \hat{R}) - \lambda \hat{R}] \right\}$$

$$= \inf_{\pi \in \Pi_P} \left\{ \mathbb{E}_{(R, \hat{R}) \sim \pi} \left[c(R, \hat{R}) - \lambda \hat{R} \right] \right\}.$$

From (A.3), we have

$$\begin{aligned} L(y) &= \sup_{\lambda \geq 0} \{ \lambda y + G(\lambda) \} \\ &= \sup_{\lambda \geq 0} \left\{ \lambda y + \inf_{\pi \in \Pi_P} \mathbb{E}_{(R, \hat{R}) \sim \pi} \left[c(R, \hat{R}) - \lambda \hat{R} \right] \right\} \\ &= \sup_{\lambda \geq 0} \left\{ \lambda y - \sup_{\pi \in \Pi_P} \mathbb{E}_{(R, \hat{R}) \sim \pi} \left[\lambda \hat{R} - c(R, \hat{R}) \right] \right\} \\ &= \sup_{\lambda \geq 0} \{ \lambda y - \mathbb{E}_P[\psi_\lambda(R)] \}, \end{aligned}$$

where the last equality comes from Lemma 2. \square

For completeness, we also include standard duality results in the literature [75, 130, 40, 50] of the worst-case risk $\mathbb{E}_Q[R]$ when Q belongs to an ambiguity set parametrized by $\rho > 0$.

Proposition 3. *We have*

$$\sup_Q \{ \mathbb{E}_Q[R] : D_{\text{kl}}(Q \| P) \leq \rho \} = \inf_{\lambda > 0} \left\{ \lambda \rho + \lambda \log \mathbb{E}_P \left[e^{\frac{R}{\lambda}} \right] \right\}, \quad (\text{A.4})$$

$$\sup_Q \{ \mathbb{E}_Q[R] : D_f(Q \| P) \leq \rho \} = \inf_{\lambda > 0, \eta \in \mathbb{R}} \left\{ \lambda \rho + \eta + \mathbb{E}_P \left[\lambda f^* \left(\frac{R - \eta}{\lambda} \right) \right] \right\}, \quad (\text{A.5})$$

$$\sup_Q \{ \mathbb{E}_Q[R] : W_c(Q, P) \leq \rho \} = \inf_{\lambda \geq 0} \{ \lambda \rho + \mathbb{E}_P[\phi_\lambda(R)] \}, \quad (\text{A.6})$$

where $\phi_\lambda(z) = \sup_{x \in \mathcal{X}} \{ x - \lambda c(z, x) \}$.

B Proof of convergence results

We begin by proving Theorem 1 in Section B.1. In Theorem 1, if we set $\bar{\lambda}$ and β to be arbitrarily close to λ^* and $\min\{2, \frac{\sigma}{\lambda}\}$ respectively, then we can obtain a convergence rate close to $O_p(n^{\min\{2, \frac{\sigma}{\lambda^*}\}^{-1}-1})$. Roughly speaking, this is the asymptotic—*distribution-dependent*—rate of convergence for the dual plug-in estimator shown by Feuerverger [47]. Unlike our finite sample convergence result, an asymptotic result requires $R^a e^{\lambda R}$ to be regularly varying of order $\frac{\lambda}{\sigma}$ [46, 33] for any $a, \lambda \geq 0$.

B.1 Proof of Theorem 1

Preliminaries Let $1 < \beta \leq \min\{2, \frac{\sigma}{\lambda}\}$, and thus $\beta \in (1, 2]$. Throughout this section, we will abuse notation and use K to denote different universal constants. Furthermore, we ignore all measurability issues in this proof which can be dealt with by using outer measures and appropriate versions of Fubini's theorems as in [142, Section 2.3]. Throughout our proof, we use the inequality $(x + y)^\beta \leq 2^{\beta-1}(x^\beta + y^\beta)$ for $x, y \geq 0$ without justification. The inequality is a consequence of convexity of $t \mapsto t^\beta$ on \mathbb{R}_+ .

Recall the ψ -Orlicz norms of a random variable R

$$\|Z\|_\psi = \inf \left\{ c > 0 : \mathbb{E} \left[\psi \left(\frac{|Z|}{c} \right) \right] \leq 1 \right\},$$

where ψ is a nondecreasing, convex function with $\psi(0) = 0$. For example, $x \mapsto x^p$ with $p \geq 1$ yields the familiar L_p -norm $\|Z\|_p = (\mathbb{E}|Z|^p)^{1/p}$. If we let $\psi_p(x) = e^{x^p} - 1$ for $p \geq 1$, we have $\|Z\|_\beta \leq \|Z\|_2 \leq \|Z\|_{\psi_2}$ since $\beta \leq 2$ and $x^2 \leq \psi_2(x)$ for $x \geq 0$.

Symmetrization In the following, we show that

$$\mathbb{E}|I(P) - \widehat{I}_n|^\beta \leq K \bar{\lambda}^\beta n^{-\beta+1} \mathbb{E}[|R|^\beta e^{\bar{\lambda}\beta R}]. \quad (\text{B.1})$$

Using Markov's inequality, we plug $t = (\delta)^{-\frac{1}{\beta}} K^{\frac{1}{\beta}} \bar{\lambda} n^{\frac{1}{\beta}-1} \left(\mathbb{E}[|R|^\beta e^{\bar{\lambda}\beta R}] \right)^{\frac{1}{\beta}}$ into $\mathbb{P} \left(|I(P) - \widehat{I}_n| \geq t \right) \leq \frac{\mathbb{E}|I(P) - \widehat{I}_n|^\beta}{t^\beta}$ and obtain the desired result (3.1).

To show the bound (B.1), define $\lambda^* := \operatorname{argmax}_\lambda \{ \lambda y - \log \mathbb{E} e^{\lambda R} \}$. Since $\mathbb{E}[R] \leq y$ and $\lambda^* \leq \bar{\lambda}$, we have $0 \leq \lambda^* \leq \bar{\lambda}$ and $I = \sup_{\lambda \in [0, \bar{\lambda}]} \{ \lambda y - \log \mathbb{E}[e^{\lambda R}] \}$. Recalling $|\log x - \log y| \leq |x - y|$ for $x, y \geq 1$, note $\mathbb{E}_{\widehat{P}_n}[e^{\lambda R}]$, $\mathbb{E}[e^{\lambda R}] \geq 1$ for $\lambda \geq 0$ to arrive at the bound

$$|I - \widehat{I}_n| \leq \sup_{\lambda \in [0, \bar{\lambda}]} \left| \log \frac{\mathbb{E}[e^{\lambda R}]}{\mathbb{E}_{\widehat{P}_n}[e^{\lambda R}]} \right| \leq \sup_{\lambda \in [0, \bar{\lambda}]} \left| \mathbb{E}[e^{\lambda R}] - \mathbb{E}_{\widehat{P}_n}[e^{\lambda R}] \right|.$$

We proceed via a symmetrization argument [142, Chapter 2.3]. Letting ε_i be i.i.d. random signs taking values in $\{-1, +1\}$ uniformly, our goal is to replace the preceding supremum with a supremum over the *symmetrized process* $\sup_{\lambda \in [0, \bar{\lambda}]} \left| \frac{1}{n} \sum_{i=1}^n \varepsilon_i e^{\lambda R_i} \right|^\beta$. We will shortly see that this latter supremum can be controlled by using the modulus of continuity of the symmetrized process $\lambda \mapsto \frac{1}{n} \sum_{i=1}^n \varepsilon_i e^{\lambda R_i}$. To this end, define R'_i to be i.i.d. copies of R_i and denote by $\mathbb{E}_{R'}$ expectation with respect to only R' . Rewrite the preceding display with this new representation

$$\begin{aligned} \mathbb{E}|I - \widehat{I}_n|^\beta &\leq \mathbb{E}_R \sup_{\lambda \in [0, \bar{\lambda}]} \left| \mathbb{E}[e^{\lambda R}] - \mathbb{E}_{\widehat{P}_n}[e^{\lambda R}] \right|^\beta = n^{-\frac{\beta}{2}} \mathbb{E}_R \sup_{\lambda \in [0, \bar{\lambda}]} \left| \mathbb{E}_{R'} \frac{1}{\sqrt{n}} \sum_{i=1}^n (e^{\lambda R_i} - e^{\lambda R'_i}) \right|^\beta \\ &\leq n^{-\frac{\beta}{2}} \mathbb{E} \sup_{\lambda \in [0, \bar{\lambda}]} \left| \frac{1}{\sqrt{n}} \sum_{i=1}^n (e^{\lambda R_i} - e^{\lambda R'_i}) \right|^\beta. \end{aligned}$$

For any set of signs ε_i , the expectation remains unchanged if we replace $e^{\lambda R_i} - e^{\lambda R'_i}$ with $\varepsilon_i(e^{\lambda R_i} - e^{\lambda R'_i})$. Using the independence of ε_i 's, conclude

$$\begin{aligned} \mathbb{E} \sup_{\lambda \in [0, \bar{\lambda}]} \left| \frac{1}{\sqrt{n}} \sum_{i=1}^n (e^{\lambda R_i} - e^{\lambda R'_i}) \right|^\beta &= \mathbb{E} \sup_{\lambda \in [0, \bar{\lambda}]} \left| \frac{1}{\sqrt{n}} \sum_{i=1}^n \varepsilon_i (e^{\lambda R_i} - e^{\lambda R'_i}) \right|^\beta \\ &\leq 2^\beta \mathbb{E} \sup_{\lambda \in [0, \bar{\lambda}]} \left| \frac{1}{\sqrt{n}} \sum_{i=1}^n \varepsilon_i e^{\lambda R_i} \right|^\beta. \end{aligned} \quad (\text{B.2})$$

For a rigorous treatment of measurability issues arising in a symmetrization argument, see van der Vaart and Wellner [142, Section 2.3].

We now bound (B.2) with a ψ_2 -Orlicz norm over the suprema of the symmetrized process. From

convexity of $t \mapsto t^\beta$ for $t \geq 0$,

$$\begin{aligned} \mathbb{E}_\epsilon \sup_{\lambda \in [0, \bar{\lambda}]} \left| \frac{1}{\sqrt{n}} \sum_{i=1}^n \epsilon_i e^{\lambda R_i} \right|^\beta &\leq 2^{\beta-1} \left(\mathbb{E}_\epsilon \sup_{\lambda \in [0, \bar{\lambda}]} \left| \frac{1}{\sqrt{n}} \sum_{i=1}^n \epsilon_i (e^{\lambda R_i} - 1) \right|^\beta + \mathbb{E}_\epsilon \left| \frac{1}{\sqrt{n}} \sum_{i=1}^n \epsilon_i \right|^\beta \right) \\ &\leq 2^{\beta-1} \left(\mathbb{E}_\epsilon \sup_{\lambda, \lambda' \in [0, \bar{\lambda}]} \left| \frac{1}{\sqrt{n}} \sum_{i=1}^n \epsilon_i (e^{\lambda R_i} - e^{\lambda' R_i}) \right|^\beta + \mathbb{E}_\epsilon \left| \frac{1}{\sqrt{n}} \sum_{i=1}^n \epsilon_i \right|^\beta \right). \end{aligned}$$

Recalling the Orlicz norm discussed in the preliminaries, the preceding display can be bounded by the ψ_2 -Orlicz norm (defined conditional on R_i)

$$2^{\beta-1} \left(\left\| \sup_{\lambda, \lambda' \in [0, \bar{\lambda}]} \left| \frac{1}{\sqrt{n}} \sum_{i=1}^n \epsilon_i (e^{\lambda R_i} - e^{\lambda' R_i}) \right| \right\|_{\psi_2}^\beta + \mathbb{E}_\epsilon \left| \frac{1}{\sqrt{n}} \sum_{i=1}^n \epsilon_i \right|^\beta \right). \quad (\text{B.3})$$

We proceed by bounding the two terms separately.

Bounding the second term in Eq. (B.3) To control $\mathbb{E}_\epsilon \left| \frac{1}{\sqrt{n}} \sum_{i=1}^n \epsilon_i \right|^\beta$, use Hoeffding's bound to get

$$\mathbb{E}_\epsilon \left| \sum_{i=1}^n \epsilon_i x_i \right|^\beta = \int_0^\infty \mathbb{P} \left(\left| \sum_{i=1}^n \epsilon_i x_i \right| \geq t \right) dt \leq \int_0^\infty 2 \exp \left(-\frac{t^\beta}{2 \|x\|_2^\beta} \right) dt = \beta 2^{\frac{\beta}{2}} \|x\|_2^\beta \int_0^\infty u^{\frac{\beta}{2}-1} e^{-u} du,$$

where we used a change of variables $u = \frac{t^\beta}{2 \|x\|_2^\beta}$. Applying this bound with $x \equiv 1$,

$$\mathbb{E}_\epsilon \left| \frac{1}{\sqrt{n}} \sum_{i=1}^n \epsilon_i \right|^\beta \leq \beta 2^{\frac{\beta}{2}} \Gamma \left(\frac{\beta}{2} \right). \quad (\text{B.4})$$

Bounding the first term in Eq. (B.3) through chaining We use a standard chaining argument (see, for example, [142, Ch. 2.2]) to control the first term in the bound (B.3). Our argument relies on the notion of covering numbers. Let $V \subset \mathcal{V}$ be any subset of a vector space \mathcal{V} . For a (semi) norm d on \mathcal{V} , we say a collection of $v_1, \dots, v_N \subset \mathcal{V}$ is an ϵ -cover of \mathcal{V} if for each $v \in \mathcal{V}$, there exists v_i such that $d(v, v_i) \leq \epsilon$. Then *covering number* of V with respect to d is given by

$$N(V, \epsilon, d) := \inf \{ N \in \mathbb{N} : \text{there is an } \epsilon\text{-cover over } V \text{ of size } N \text{ with respect to } d \}.$$

The following classical chaining inequality bounds the ψ_2 -Orlicz norm of the supremum of a stochastic process.

Lemma 3. [142, Theorem 2.2.4] *For some (semi) metric d on V , let $\{Z_v : v \in V\}$ be a separable stochastic process with*

$$\|Z_v - Z_w\|_{\psi_2} \leq C d(v, w) \quad \text{for every } v, w \in V$$

for a constant C . Then, for a constant K depending only on C

$$\left\| \sup_{v, w \in V} |Z_v - Z_w| \right\|_{\psi_2} \leq K \int_0^{\text{diam } V} \sqrt{\log N(V, \epsilon, d)} d\epsilon.$$

To apply Lemma 3, we verify $\lambda \mapsto \frac{1}{\sqrt{n}} \sum_{i=1}^n \varepsilon_i e^{\lambda R_i}$ is Lipschitz with respect to the $L_2(\widehat{P}_n)$ -norm $\|Z\|_n := \left(\frac{1}{n} \sum_{i=1}^n Z_i^2\right)^{\frac{1}{2}}$. Conditional on R_i 's, Hoeffding's inequality gives

$$\mathbb{P}_\varepsilon \left(\left| \frac{1}{\sqrt{n}} \sum_{i=1}^n \varepsilon_i e^{\lambda R_i} - \frac{1}{\sqrt{n}} \sum_{i=1}^n \varepsilon_i e^{\lambda' R_i} \right| \geq t \right) \leq 2 \exp \left(-\frac{t^2}{2 \|e^{\lambda R} - e^{\lambda' R}\|_n^2} \right).$$

Claim 4. *The preceding display implies*

$$\left\| \frac{1}{\sqrt{n}} \sum_{i=1}^n \varepsilon_i e^{\lambda R_i} - \frac{1}{\sqrt{n}} \sum_{i=1}^n \varepsilon_i e^{\lambda' R_i} \right\|_{\psi_2} \leq \sqrt{6} \|e^{\lambda R} - e^{\lambda' R}\|_n.$$

Proof of Claim For any random variable Z such that $\mathbb{P}(|Z| > u) \leq 2 \exp(-v^2 u^2)$, Fubini gives

$$\mathbb{E}[e^{(Z/c)^2} - 1] = \int_0^\infty \mathbb{P} \left(e^{(Z/c)^2} - 1 \geq t \right) dt = \int_0^\infty \mathbb{P} (|Z| \geq \sqrt{u}) \frac{1}{c^2} e^{u/c^2} du \leq \frac{2}{c^2 v - 1}$$

where we used the change of variables $u = c^2 \log(t + 1)$. Since $2/(c^2 v - 1) \leq 1$ for $c \geq \sqrt{3/v}$, we obtain the claim. \square

Letting $\mathcal{F} := \{x \mapsto e^{\lambda x} : \lambda \in [0, \bar{\lambda}]\}$, use the claim to apply Lemma 3, which immediately yields

$$\begin{aligned} \left\| \sup_{\lambda, \lambda' \in [0, \bar{\lambda}]} \left| \frac{1}{\sqrt{n}} \sum_{i=1}^n \varepsilon_i (e^{\lambda R_i} - e^{\lambda' R_i}) \right| \right\|_{\psi_2} &\leq K \int_0^{\bar{\lambda} \|F\|_n} \sqrt{\log N(\varepsilon, \mathcal{F}, \|\cdot\|_n)} d\varepsilon \\ &= K \int_0^{\bar{\lambda}} \sqrt{\log N(\varepsilon \|F\|_n, \mathcal{F}, \|\cdot\|_n)} d\varepsilon \cdot \|F\|_n. \end{aligned}$$

To bound the covering number of \mathcal{F} , we use the Lipschitzness of $\lambda \mapsto e^{\lambda x}$.

Lemma 5. [142, Theorem 2.7.11] *If $\mathcal{F} = \{f_\lambda : \lambda \in \Lambda\}$ is a class of functions such that $|f_\lambda(x) - f_{\lambda'}(x)| \leq F(x)d(\lambda, \lambda')$ for some metric d on Λ and function F on the sample space, we have*

$$N(\varepsilon \|F\|, \mathcal{F}, \|\cdot\|_n) \leq N(\varepsilon, \Lambda, d).$$

Note that $|e^{\lambda x} - e^{\lambda' x}| \leq F(x)|\lambda - \lambda'|$ with $F(x) = x e^{\bar{\lambda} x}$. Applying Lemma 5 with $\Lambda := [0, \bar{\lambda}]$,

$$\int_0^{\bar{\lambda}} \sqrt{\log N(\varepsilon \|F\|_n, \mathcal{F}, L_2(\widehat{P}_n))} d\varepsilon \cdot \|F\|_n \leq \int_0^{\bar{\lambda}} \sqrt{\log \left(1 + \frac{\bar{\lambda}}{\varepsilon} \right)} d\varepsilon \cdot \|F\|_n \leq K \bar{\lambda} \|F\|_n.$$

Final bound Collecting these bounds, we arrive at

$$\mathbb{E}|I - \widehat{I}_n|^\beta \leq 2^{2\beta-1} n^{-\frac{\beta}{2}} \mathbb{E}_{R, \varepsilon} \sup_{\lambda \in [0, \bar{\lambda}]} \left| \frac{1}{\sqrt{n}} \sum_{i=1}^n \varepsilon_i e^{\lambda R_i} \right|^\beta \leq 2^{2\beta-1} n^{-\frac{\beta}{2}} \left(K \bar{\lambda}^\beta \mathbb{E}_R [\|F\|_n^\beta] + \beta 2^{\frac{\beta}{2}} \Gamma \left(\frac{\beta}{2} \right) \right).$$

Noting $\|x\|_1 \leq (\sum_{i=1}^n |x_i|^{\beta/2})^{2/\beta}$ for $\beta \in (1, 2]$, the final result (B.1) follows from

$$\mathbb{E}_R \|F\|_n^\beta = n^{-\frac{\beta}{2}} \mathbb{E}_R \left(\sum_{i=1}^n R_i^2 e^{2\bar{\lambda} R_i} \right)^{\frac{\beta}{2}} \leq n^{-\frac{\beta}{2}+1} \mathbb{E}[|R|^\beta e^{\bar{\lambda} \beta R}].$$

Summarizing, we have shown

$$\begin{aligned}
\mathbb{E}|I - \widehat{I}_n|^\beta &\leq 2^{2\beta-1} n^{-\frac{\beta}{2}} \mathbb{E}_{R,\epsilon} \sup_{\lambda \in [0, \bar{\lambda}]} \left| \frac{1}{\sqrt{n}} \sum_{i=1}^n \epsilon_i e^{\lambda R_i} \right|^\beta \\
&\leq 2^{2\beta-1} n^{-\frac{\beta}{2}} \left(K \bar{\lambda}^\beta \mathbb{E}_R [\|F\|_n^\beta] + \beta 2^{\frac{\beta}{2}} \Gamma\left(\frac{\beta}{2}\right) \right) \\
&\leq K \bar{\lambda}^\beta n^{-\beta+1} \mathbb{E} [|R|^\beta e^{\bar{\lambda} \beta R}].
\end{aligned} \tag{B.5}$$

for an appropriately large universal constant K , which is exactly (B.1).

B.2 Proof of Theorem 2

For an $\epsilon > 0$ to be chosen later, let $\bar{\lambda} = \sigma - \frac{\alpha}{y}$ and $\beta := \frac{1}{1+2\epsilon} \frac{\sigma}{\sigma - \alpha/y} \in (1, 2)$. Applying Theorem 1 with this definition of $\bar{\lambda}$ and β , we proceed to bound $\mathbb{E}_P [R^\beta e^{\bar{\lambda} \beta R}]$ uniformly over $P \in \mathcal{P}_{\sigma, y, \alpha}$.

Toward this goal, we will use the following useful algebraic inequality

$$x^a \leq e^{tx} \left(\frac{a}{et}\right)^a \quad \text{for all } x \geq 0, t > 0, a > 0. \tag{B.6}$$

To see this, note that $1 + y \leq e^y$ with $y = -1 + \frac{tx}{a}$ gives $\frac{tx}{a} \leq e^{\frac{tx}{a} - 1}$. Applying the inequality (B.6) with $t = \frac{\epsilon}{1+2\epsilon} \sigma$, $a = \beta$, we deduce

$$R^\beta e^{\bar{\lambda} \beta R} \leq e^{\frac{1}{1+2\epsilon} \sigma R} e^{\frac{\epsilon}{1+2\epsilon} \sigma R} \left(\frac{\beta}{e}\right)^\beta \left(\frac{1+2\epsilon}{\epsilon \sigma}\right)^\beta.$$

Taking expectation on both sides, use Condition 2 and $\beta < e$ to arrive at

$$\mathbb{E}_P [R^\beta e^{\bar{\lambda} \beta R}] \leq \left(\frac{\beta}{e}\right)^\beta \left(\frac{1+2\epsilon}{\epsilon \sigma}\right)^\beta \mathbb{E}_P \left[e^{\frac{1+2\epsilon}{1+2\epsilon} \sigma R} \right] \leq \left(\frac{1+2\epsilon}{\epsilon}\right)^{\beta+1} \left(\frac{1}{\sigma}\right)^\beta. \tag{B.7}$$

Using the preceding bound on $\mathbb{E}_P [R^\beta e^{\bar{\lambda} \beta R}]$ in Theorem 1, conclude

$$\sup_{P \in \mathcal{P}_{\sigma, y, \alpha}} \mathbb{P} \left(\left| \widehat{I}_n - I(P) \right| \geq K \left(1 - \frac{\alpha}{\sigma y}\right) \left(\frac{1}{\delta}\right)^{(1+2\epsilon)(1 - \frac{\alpha}{\sigma y})} \left(2 + \frac{1}{\epsilon}\right)^{1+(1+2\epsilon)(1 - \frac{\alpha}{\sigma y})} n^{-\frac{\alpha}{\sigma y} + 2\epsilon(1 - \frac{\alpha}{\sigma y})} \right) \leq \delta.$$

Choose $\epsilon := \frac{1}{2 \log n} \frac{1}{1 - \frac{\alpha}{\sigma y}}$. Noting that $\epsilon \leq \frac{1}{2}$ since $n \geq 8 > e^2 \geq \exp\left(\frac{1}{1 - \frac{\alpha}{\sigma y}}\right)$ and $n^{1/\log n} = e$, we obtain the desired result.

B.3 Proof of Theorem 3

Applying Theorem 1 with $\bar{\lambda} := \sigma - \frac{\alpha}{y}$ and $\beta = 2$, it remains to bound $\mathbb{E}_P [R^\beta e^{\bar{\lambda} \beta R}]$ uniformly over $P \in \mathcal{P}_{\sigma, y, \alpha}$. Use the bound (B.6) with $t = \frac{\alpha}{y} - \frac{\sigma}{2} > 0$ and note $a = 2 < e$ to get

$$R^\beta e^{\bar{\lambda} \beta R} \leq e^{2(\sigma - \frac{\alpha}{y})R} e^{(\frac{\alpha}{y} - \frac{\sigma}{2})R} \left(\frac{1}{\frac{\alpha}{y} - \frac{\sigma}{2}}\right)^2.$$

Taking expectation on both sides and using Condition 2,

$$\mathbb{E}_P [R^\beta e^{\bar{\lambda} \beta R}] \leq \left(\frac{y}{\alpha - \frac{\sigma y}{2}}\right)^2 \frac{\sigma y}{\alpha - \frac{\sigma y}{2}}. \tag{B.8}$$

B.4 Proof of Theorem 4

We use the same proof as in Theorem 2, except that we change (B.7) to

$$\mathbb{E}_P[R^\beta e^{\bar{\lambda}\beta R}] \leq \left(\frac{\beta}{e}\right)^\beta \left(\frac{1+2\epsilon}{\epsilon\sigma}\right)^\beta \mathbb{E}_P \left[e^{\frac{1+\epsilon}{1+2\epsilon}\sigma R} \right] \leq \left(\frac{1+2\epsilon}{\epsilon}\right)^{\beta+m} \left(\frac{1}{\sigma}\right)^\beta.$$

and then the rest follows similarly, and we complete proving (3.5).

B.5 Proof of properties of $\mathcal{Q}_{\bar{\lambda},y}$

The statement for Gaussian random variables follows directly from Example 2.

We now consider $P = \text{Ber}(p)$, then $F(\lambda) := \lambda y - \log \mathbb{E}_P[e^{\lambda R}] = \lambda y - \log((1-p) + pe^\lambda)$ and $F'(\lambda) = y - \frac{pe^\lambda}{1-p+pe^\lambda}$, so we obtain $\lambda^* = \log\left(\frac{(1-p)y}{p(1-y)}\right)$ by setting $F'(\lambda) = 0$. Solving $\lambda^* \leq \bar{\lambda}$ yields $p \geq \frac{y}{e^{\bar{\lambda}-y}(e^{\bar{\lambda}}-1)}$.

Next, consider $P = \text{Uni}(0, 1)$, we have $F(\lambda) = \lambda y - \log\left(\frac{e^\lambda-1}{\lambda}\right)$, then

$$F'(\lambda) = \frac{e^\lambda((y-1)\lambda+1) - y\lambda - 1}{\lambda e^\lambda - 1}.$$

Noting that $F'(\frac{1}{1-y}) \leq 0$, we have $\lambda^*(\text{Uni}(0, 1)) \leq \frac{1}{1-y}$. Similarly, we can show that $\lambda^*(\text{Uni}(0, b)) \leq \frac{1}{1-y/b}$ and $\lambda^*(\text{Uni}(a, b)) \leq \frac{1}{1-(y-a)/(b-a)} = \frac{b-a}{b-y}$.

C Proof of fundamental hardness results

C.1 Proof of Theorem 5

We proceed by using Le Cam's method by reducing the estimation problem to a binary hypothesis test. We denote by \mathcal{P} the set of probability distributions over which the worst-case is taken over.

Lemma 6 (Lemma 1, Yu [155]). *Let (Θ, d) be a pseudo-metric space and let $\theta : \mathcal{P} \rightarrow \Theta$ be the parameter of interest. If there exists $P_1, P_2 \in \mathcal{P}$ such that $d(\theta(P_1), \theta(P_2)) \geq 2\epsilon$, we have*

$$\inf_{\hat{\theta}(R_1^n)} \sup_{P \in \mathcal{P}} \mathbb{P} \left(d(\hat{\theta}(R_1^n), \theta(P)) \geq \epsilon \right) \geq \frac{1}{2} (1 - \|P_1^n - P_2^n\|_{\text{TV}}).$$

We take $\theta(P) = I(P)$, $d(I(P_1), I(P_2)) = |I(P_1) - I(P_2)|$ and $\mathcal{P} = \mathcal{P}_{\sigma, y, \alpha}$. To apply the lemma, we construct two distributions P_1 and P_2 that are well-separated in terms of $I(P_i)$ but are close in total variation distance.

Our example is inspired by Hall et al. [64, Theorem 3]. Let $1 < x_0$ be some fixed number to be chosen later. Throughout the section, we set $\eta := 1 - \alpha - \frac{1}{\sigma x_0}$ and define $R_1 \sim P_1 = \text{Gamma}(1 - \eta, \sigma) = \text{Gamma}(\alpha + \frac{1}{\sigma x_0}, \sigma)$ with density $f_1(x) = \frac{\sigma^{1-\eta}}{\Gamma(1-\eta)} x^{-\eta} e^{-\sigma x} \mathbf{1}\{x \geq 0\}$ and $R_2 \sim P_2$ with density

$$f_2(x) = \begin{cases} 0 & \text{if } x < 0 \\ \frac{\sigma^{1-\eta}}{\Gamma(1-\eta)} x^{-\eta} e^{-\sigma x} & \text{if } 0 \leq x \leq x_0 \\ C x^{-1} e^{-\sigma x} & \text{if } x > x_0 \end{cases} \quad \text{where } C := \frac{\frac{\sigma^{1-\eta}}{\Gamma(1-\eta)} \int_{x_0}^{\infty} x^{-\eta} e^{-\sigma x} dx}{\int_{x_0}^{\infty} x^{-1} e^{-\sigma x} dx}.$$

Throughout this section, we assume $y \geq \mathbb{E}[R_1]$ and $y \geq \mathbb{E}[R_2]$.

Since $\sigma x_0 \geq \frac{2}{1-\alpha} \geq \frac{2}{\alpha}$, $\frac{1}{2}(1-\alpha) \leq \eta \leq 1-\alpha$ and $\alpha \leq 1-\eta \leq \frac{3}{2}\alpha$. We also have

$$\frac{1}{\Gamma(\alpha)} \leq \frac{1}{\Gamma(1-\eta)} \leq 1, \quad \alpha - 1 \leq -\eta \leq \frac{1}{2}(\alpha - 1). \quad (\text{C.1})$$

We will use the following estimate repeatedly. From integration by parts,

$$\int_{x_0}^{\infty} \frac{1}{x^\eta} e^{-x} dx = \frac{1}{x_0^\eta} e^{-x_0} - \eta \int_{x_0}^{\infty} \frac{1}{x^{\eta+1}} e^{-x} dx = \frac{1}{x_0^\eta} e^{-x_0} - \eta \frac{1}{x_0^{\eta+1}} e^{-x_0} + \eta(\eta+1) \int_{x_0}^{\infty} \frac{1}{x^{\eta+2}} e^{-x} dx,$$

so that for any $w > 0$

$$e^{-wx_0} \frac{1}{wx_0^\eta} \left(1 - \frac{\eta}{wx_0}\right) \leq \int_{x_0}^{\infty} \frac{1}{x^\eta} e^{-wx} dx \leq e^{-wx_0} \frac{1}{wx_0^\eta} \left(1 \wedge \left(1 - \eta \frac{1}{wx_0} + \eta(\eta+1) \frac{1}{w^2 x_0^2}\right)\right). \quad (\text{C.2})$$

In particular, we have

$$\frac{\sigma^{1-\eta}}{\Gamma(1-\eta)} x_0^{1-\eta} \left(1 - \frac{\eta}{\sigma x_0}\right) \leq C \leq \frac{\sigma^{1-\eta}}{\Gamma(1-\eta)} x_0^{1-\eta} \left(1 + \frac{1}{\sigma x_0 - 1}\right). \quad (\text{C.3})$$

We first confirm P_1 and P_2 are included in the set under consideration. See Section C.1.1 for the proof.

Lemma 7. $P_1, P_2 \in \mathcal{P}_{\sigma, y, \alpha}$ if

$$x_0 \geq \frac{y}{\alpha} \left(2 \log x_0 + \log \left(\frac{4\sigma \left(\frac{\alpha}{y} \vee 1\right)}{1-\alpha}\right)\right) \vee 2.$$

Next, we show $I_1 = I(P_1)$ and $I_2 = I(P_2)$ are well-separated.

Lemma 8. Let $\sigma y \geq 2\alpha$. If $x_0 \geq \left(\frac{2}{\alpha^2} \frac{\sigma y + 1}{\sigma y - 1} \vee \frac{2}{\alpha} \vee \frac{4}{\sigma y - 1}\right) y$, we have

$$|I_1 - I_2| = I_2 - I_1 \geq \frac{1}{\Gamma(\alpha)} \left(\frac{y}{x_0}\right)^{1-\alpha} e^{-(1-\eta)x_0/y} \frac{\sigma y - 1}{2(\sigma y + 1)(\sigma x_0 - 1)}.$$

We defer the proof of the lemma to Section C.1.2.

Finally, we wish to show P_1 and P_2 are close in total variation distance despite being well-separated in $I(P)$. From Pinsker's inequality, we have $\|P_1^n - P_2^n\|_{\text{TV}}^2 \leq \frac{1}{2} D_{\text{kl}}(P_1^n \| P_2^n) = \frac{n}{2} D_{\text{kl}}(P_1 \| P_2)$. See Section C.2 for a proof of the following bound on the KL divergence.

Lemma 9. If $x_0 \geq \frac{\log 3(1 \vee \sigma^{-2})}{\frac{1}{2}(1-\alpha)}$ and $x_0 \geq 1 + \frac{1}{\sigma}$, then $D_{\text{kl}}(P_1 \| P_2) \leq e^{-\sigma x_0}$.

Let $x_0 = \frac{1}{\sigma} \log cn$ for $c = \frac{1}{2(1-2\delta)^2}$. By Lemma 9, we have $D_{\text{kl}}(P_1 \| P_2) \leq e^{-\sigma x_0} = \frac{1}{cn}$ and $\|P_1^n - P_2^n\|_{\text{TV}} \leq 1 - 2\delta$. Applying Lemmas 6, 8, and using the identity

$$e^{-(1-\eta)x_0/y} = \left(\frac{1}{cn}\right)^{\frac{1-\eta}{\sigma y}} = \left(\frac{1}{cn}\right)^{\frac{\alpha + \frac{1}{\log cn}}{\sigma y}} = \left(\frac{1}{cn}\right)^{\frac{\alpha}{\sigma y}} e^{-\frac{1}{\sigma y}},$$

we obtain $\mathfrak{M}_n \geq \delta$ as claimed in Theorem 5.

C.1.1 Proof of Lemma 7

First, we show that $P_1 \in \mathcal{P}_{\sigma, y, \alpha}$. Since $\mathbb{E}e^{\lambda R_1} = \left(\frac{\sigma}{\sigma - \lambda}\right)^{1-\eta} \leq \frac{\sigma}{\sigma - \lambda}$, $\mathbb{E}[R_1] = \frac{1-\eta}{\sigma} < \frac{1}{\sigma}$, and $\lambda^*(P_1) = \sigma - (1-\eta)/y \leq \sigma - \frac{\alpha}{y}$, all conditions are satisfied.

Clearly, R_2 satisfies Condition 1. To confirm that Condition 2 is satisfied, we first present an integral inequality that is similar to the well-known covariance inequality (Proposition 7.2.1, [126]): $\mathbb{E}[f(R)g(R)] \geq \mathbb{E}[f(R)]\mathbb{E}[g(R)]$ for any increasing functions f, g and random variable R .

Lemma 10 (Theorem 1, [151]). *Consider four non-negative functions f_1, f_2, g_1, g_2 , an interval $A \subset \mathbb{R}$, and assume $\int_A f_i g_j d\mu > 0$ for $i, j = 1, 2$. If $\frac{f_1}{f_2}$ and $\frac{g_1}{g_2}$ are monotonic in the same direction, then*

$$\frac{\int_A f_1 g_1 d\mu}{\int_A f_1 g_2 d\mu} \geq \frac{\int_A f_2 g_1 d\mu}{\int_A f_2 g_2 d\mu}.$$

Proof Define $F(x, y) = f_1(x)f_2(y) - f_1(y)f_2(x)$, $G(x, y) = g_1(x)g_2(y) - g_1(y)g_2(x)$. Since $\frac{f_1}{f_2}$ and $\frac{g_1}{g_2}$ are monotonic in the same direction, we deduce $F(x, y)G(x, y) \geq 0$ and

$$\int_A f_1 g_1 d\mu \int_A f_2 g_2 d\mu - \int_A f_1 g_2 d\mu \int_A f_2 g_1 d\mu = \frac{1}{2} \int_A \int_A F(x, y)G(x, y) \mu(dx) \mu(dy) \geq 0.$$

□

By Lemma 10 with $f_1(x) = e^{-(\sigma-\lambda)x}$, $f_2(x) = e^{-\sigma x}$, $g_1(x) = x^{-\eta}$, $g_2(x) = x^{-1}$, we have

$$\frac{\int_{x_0}^{\infty} x^{-\eta} e^{-\sigma x} dx}{\int_{x_0}^{\infty} x^{-1} e^{-\sigma x} dx} \leq \frac{\int_{x_0}^{\infty} x^{-\eta} e^{-(\sigma-\lambda)x} dx}{\int_{x_0}^{\infty} x^{-1} e^{-(\sigma-\lambda)x} dx},$$

so that

$$\begin{aligned} \mathbb{E}[e^{\lambda R_2}] &= \int_0^{x_0} \frac{\sigma^{1-\eta}}{\Gamma(1-\eta)} x^{-\eta} e^{-(\sigma-\lambda)x} dx + \int_{x_0}^{\infty} \frac{\sigma^{1-\eta}}{\Gamma(1-\eta)} \frac{\int_{x_0}^{\infty} x^{-\eta} e^{-\sigma x} dx}{\int_{x_0}^{\infty} x^{-1} e^{-\sigma x} dx} x^{-1} e^{-(\sigma-\lambda)x} dx \\ &\leq \int_0^{x_0} \frac{\sigma^{1-\eta}}{\Gamma(1-\eta)} x^{-\eta} e^{-(\sigma-\lambda)x} dx + \int_{x_0}^{\infty} \frac{\sigma^{1-\eta}}{\Gamma(1-\eta)} x^{-\eta} e^{-(\sigma-\lambda)x} dx \\ &= \mathbb{E}[e^{\lambda R_1}] = \left(\frac{\sigma}{\sigma - \lambda}\right)^{1-\eta} \leq \frac{\sigma}{\sigma - \lambda}. \end{aligned} \tag{C.4}$$

Similarly, Lemma 10 implies $\mathbb{E}[R_2] \leq \mathbb{E}[R_1] < \frac{1}{\sigma}$.

It now remains to show that R_2 satisfies Condition 3. By (3.2), it suffices to show $\mathbb{E}[R_2 e^{(\sigma-\alpha/y)R_2}] \geq y\mathbb{E}[e^{(\sigma-\alpha/y)R_2}]$. Before proving this, it is useful to have the following technical result.

Lemma 11. *For any $\eta > 0$, $x_0 \geq \eta + 1$, $w > 0$,*

$$\int_{x_0}^{\infty} e^{-wx} x^\eta dx \leq \frac{1}{w} (\eta + 1) e^{-wx_0} x_0^\eta. \tag{C.5}$$

Proof Let $f(x) = \eta \log x - x$ so that $e^{-x} x^\eta = e^{f(x)}$. Since f is concave for $\eta > 0$, $f(x) \leq f(x_0) + f'(x_0)(x - x_0)$ or equivalently, $\eta \log x - x \leq \eta \log x_0 - x_0 + (\eta/x_0 - 1)(x - x_0)$. Hence,

$$\int_{x_0}^{\infty} e^{-x} x^\eta dx \leq \int_{x_0}^{\infty} e^{-x_0} x_0^\eta e^{-(1-\eta/x_0)(x-x_0)} dx = e^{-x_0} x_0^\eta \frac{1}{1-\eta/x_0} \leq e^{-x_0} x_0^\eta (\eta + 1),$$

where we used $\frac{1}{1-\eta/x_0} \leq \eta + 1$ for all $x_0 \geq 1 + \eta$ in the final inequality. We have the result since $\int_{x_0}^{\infty} e^{-wx} x^\eta dx = \frac{1}{w^{1+\eta}} \int_{wx_0}^{\infty} e^{-x} x^\eta dx$. \square

Applying Lemma 11, we have

$$\begin{aligned} \mathbb{E}[R_2 e^{\lambda R_2}] &\geq \frac{\sigma^{1-\eta}}{\Gamma(1-\eta)} \int_0^{x_0} x^{1-\eta} e^{-(\sigma-\lambda)x} dx \\ &= \frac{\sigma^{1-\eta}}{\Gamma(1-\eta)} \left(\Gamma(2-\eta) \frac{1}{(\sigma-\lambda)^{2-\eta}} - \int_{x_0}^{\infty} x^{1-\eta} e^{-(\sigma-\lambda)x} dx \right) \\ &\geq \frac{\sigma^{1-\eta}}{\Gamma(1-\eta)} \left(\Gamma(2-\eta) \frac{1}{(\sigma-\lambda)^{2-\eta}} - (2-\eta) \frac{1}{\sigma-\lambda} e^{-(\sigma-\lambda)x_0} x_0^{1-\eta} \right) \\ &= \frac{\sigma^{1-\eta}}{\Gamma(1-\eta)} \frac{1}{(\sigma-\lambda)^{2-\eta}} \left(\Gamma(2-\eta) - (2-\eta)(\sigma-\lambda)^{-\eta+1} e^{-(\sigma-\lambda)x_0} x_0^{1-\eta} \right) \\ &\geq \left(\frac{\sigma}{\sigma-\lambda} \right)^{1-\eta} \frac{1}{\Gamma(1-\eta)(\sigma-\lambda)} \left(\Gamma(2-\eta) - (2-\eta)(\sigma-\lambda)^{-\eta+1} e^{-(\sigma-\lambda)x_0} x_0^{1-\eta} \right) \end{aligned}$$

Plugging in $\lambda = \sigma - \frac{\alpha}{y}$, we wish to bound the final term inside the parentheses. Recall from the line above Eq. (C.1) that $\frac{4}{1-\alpha} \geq \frac{2}{\eta} \geq \frac{2-\eta}{\eta}$ and $1 \geq \frac{1}{\Gamma(1-\eta)}$. Using these inequalities and the hypothesis,

$$x_0 \geq \frac{y}{\alpha} \left(2 \log x_0 + \log \left(\frac{4\sigma \left(\frac{\alpha}{y} \vee 1 \right)}{1-\alpha} \right) \right) \geq \frac{y}{\alpha} \left((2-\eta) \log x_0 + \log \left(\frac{(2-\eta)\sigma \left(\frac{\alpha}{y} \right)^{-\eta+1}}{\Gamma(1-\eta)\eta} \right) \right).$$

Rewriting the bound, we have

$$\frac{(2-\eta) \left(\frac{\alpha}{y} \right)^{-\eta+1} e^{-\alpha x_0/y} x_0^{1-\eta}}{\Gamma(1-\eta)} \leq \frac{1}{\sigma x_0}. \quad (\text{C.6})$$

Noting $x_0 \geq 2 > 2 - \eta$, we arrive at

$$\mathbb{E}[R_2 e^{\lambda R_2}] \geq \left(\frac{\sigma}{\sigma-\lambda} \right)^{1-\eta} \frac{1}{\sigma-\lambda} \left(1 - \eta - \frac{1}{\sigma x_0} \right) \geq \left(\frac{\sigma}{\sigma-\lambda} \right)^{1-\eta} \frac{1}{\sigma-\lambda} \alpha,$$

where we used $\frac{\Gamma(2-\eta)}{\Gamma(1-\eta)} = 1 - \eta$ and the bound (C.6) in the first inequality, and $\eta = 1 - \alpha - \frac{1}{\sigma x_0}$ in the second inequality. We conclude

$$\mathbb{E} \left[R_2 e^{\left(\sigma - \frac{\alpha}{y} \right) R_2} \right] \geq \left(\frac{\sigma y}{\alpha} \right)^{1-\eta} \frac{y}{\alpha} \alpha = y \mathbb{E} \left[e^{\left(\sigma - \frac{\alpha}{y} \right) R_1} \right] \geq y \mathbb{E} \left[e^{\left(\sigma - \frac{\alpha}{y} \right) R_2} \right],$$

where the final inequality follows from the bound (C.4).

C.1.2 Proof of Lemma 8

Plugging $\mathbb{E}[e^{\lambda R_1}] = \left(\frac{\sigma}{\sigma-\lambda} \right)^{1-\eta}$ into the expression for I_1 , we get $\lambda^*(P_1) = \sigma - \frac{1-\eta}{y}$ and

$$I_1 = \sup_{\lambda} \{ \lambda y - \kappa_1(\lambda) \} = y \left(\sigma - \frac{1-\eta}{y} \right) - \kappa_1 \left(\sigma - \frac{1-\eta}{y} \right).$$

Letting $\kappa_j(\lambda) = \log \mathbb{E}e^{\lambda R_j}$, we have the following lower bound on the separation

$$\begin{aligned}
|I_1 - I_2| &\geq I_2 - I_1 = \sup_{\lambda} \{\lambda y - \kappa_2(\lambda)\} - \sup_{\lambda} \{\lambda y - \kappa_1(\lambda)\} \\
&\geq y \left(\sigma - \frac{1-\eta}{y} \right) - \kappa_2 \left(\sigma - \frac{1-\eta}{y} \right) - \left(y \left(\sigma - \frac{1-\eta}{y} \right) - \kappa_1 \left(\sigma - \frac{1-\eta}{y} \right) \right) \\
&= \kappa_1 \left(\sigma - \frac{1-\eta}{y} \right) - \kappa_2 \left(\sigma - \frac{1-\eta}{y} \right) = \log \frac{\mathbb{E}e^{(\sigma - \frac{1-\eta}{y})R_1}}{\mathbb{E}e^{(\sigma - \frac{1-\eta}{y})R_2}} \\
&\geq \frac{\mathbb{E}e^{(\sigma - \frac{1-\eta}{y})R_1} - \mathbb{E}e^{(\sigma - \frac{1-\eta}{y})R_2}}{\mathbb{E}e^{(\sigma - \frac{1-\eta}{y})R_1}} = 1 - \left(\frac{\sigma y}{1-\eta} \right)^{\eta-1} \mathbb{E}e^{(\sigma - \frac{1-\eta}{y})R_2}, \tag{C.7}
\end{aligned}$$

where we used $\log x \geq 1 - \frac{1}{x}$ in the last inequality.

We proceed by upper bounding $\mathbb{E}e^{(\sigma - \frac{1-\eta}{y})R_2}$. Using the bounds (C.2) and (C.3), we have

$$\begin{aligned}
\int_{x_0}^{\infty} Cx^{-1}e^{-(\sigma-\lambda)x}dx &\leq C \frac{1}{\sigma-\lambda} e^{-(\sigma-\lambda)x_0} \frac{1}{x_0} \left(1 - \frac{1}{(\sigma-\lambda)x_0} + 2 \frac{1}{(\sigma-\lambda)^2 x_0^2} \right) \\
&\leq \frac{\sigma^{1-\eta}}{\Gamma(1-\eta)} \frac{\sigma x_0}{\sigma x_0 - 1} \frac{1}{\sigma - \lambda} e^{-(\sigma-\lambda)x_0} x_0^{-\eta} \left(1 - \frac{1}{(\sigma-\lambda)x_0} + 2 \frac{1}{(\sigma-\lambda)^2 x_0^2} \right),
\end{aligned}$$

and

$$\begin{aligned}
\int_0^{x_0} \frac{\sigma^{1-\eta}}{\Gamma(1-\eta)} x^{-\eta} e^{-(\sigma-\lambda)x} dx &= \left(\frac{\sigma}{\sigma-\lambda} \right)^{1-\eta} - \int_{x_0}^{\infty} \frac{\sigma^{1-\eta}}{\Gamma(1-\eta)} x^{-\eta} e^{-(\sigma-\lambda)x_0} dx \\
&\leq \left(\frac{\sigma}{\sigma-\lambda} \right)^{1-\eta} - \frac{\sigma^{1-\eta}}{\Gamma(1-\eta)} (\sigma-\lambda)^{-1} e^{-(\sigma-\lambda)x_0} x_0^{-\eta} \left(1 - \frac{\eta}{(\sigma-\lambda)x_0} \right).
\end{aligned}$$

Combining these bounds,

$$\begin{aligned}
\mathbb{E}[e^{\lambda R_2}] &\leq \left(\frac{\sigma}{\sigma-\lambda} \right)^{1-\eta} + \frac{\sigma^{1-\eta}}{\Gamma(1-\eta)} x_0^{-\eta} \frac{1}{\sigma-\lambda} e^{-(\sigma-\lambda)x_0} \\
&\quad \times \left\{ \left(1 + \frac{1}{\sigma x_0 - 1} \right) \left(1 - \frac{1}{(\sigma-\lambda)x_0} + 2 \frac{1}{(\sigma-\lambda)^2 x_0^2} \right) - 1 + \frac{\eta}{(\sigma-\lambda)x_0} \right\}.
\end{aligned}$$

Plugging $\lambda = \sigma - \frac{1-\eta}{y}$ into the final term in the preceding display, we use $x_0 \geq \left(\frac{2}{\alpha^2} \frac{\sigma y + 1}{\sigma y - 1} \vee \frac{2}{\alpha} \right) y \geq \left(\frac{2}{(1-\eta)^2} \frac{\sigma y + 1}{\sigma y - 1} \vee \frac{2}{1-\eta} \right) y$ to get

$$\begin{aligned}
&\left(1 + \frac{1}{\sigma x_0 - 1} \right) \left(1 - \frac{1}{(\sigma-\lambda)x_0} + 2 \frac{1}{(\sigma-\lambda)^2 x_0^2} \right) - 1 + \frac{\eta}{(\sigma-\lambda)x_0} \\
&= \frac{1}{\sigma x_0 - 1} \left(1 - \frac{1}{(\sigma-\lambda)x_0} + 2 \frac{1}{(\sigma-\lambda)^2 x_0^2} \right) - \frac{1}{(\sigma-\lambda)x_0} \left(1 - \eta - \frac{2}{(\sigma-\lambda)x_0} \right) \\
&\stackrel{(a)}{\leq} \frac{1}{\sigma x_0 - 1} - \frac{1}{x_0/y(1-\eta)} \left(1 - \eta - \frac{2}{(1-\eta)x_0/y} \right) \\
&\stackrel{(b)}{\leq} \frac{1}{\sigma x_0 - 1} - \frac{1}{x_0/y} \frac{2}{\sigma y + 1}
\end{aligned}$$

$$\stackrel{(c)}{\leq} \frac{2y}{(\sigma y + 1)x_0(\sigma x_0 - 1)} \left(-\frac{\sigma y - 1}{4} \frac{x_0}{y} \right) = -\frac{\sigma y - 1}{2(\sigma y + 1)(\sigma x_0 - 1)},$$

where in steps (a) and (b) we used $\frac{1}{(\sigma - \lambda)x_0} - 2\frac{1}{(\sigma - \lambda)^2 x_0^2} \leq 0$, $\frac{2}{(1 - \eta)^2 x_0/y} \leq \frac{\sigma y - 1}{\sigma y + 1}$, and in step (c) we used $x_0 \geq \frac{4}{\sigma y - 1}y$.

Collecting previous bounds, we arrive at

$$\mathbb{E}[e^{(\sigma - \frac{1 - \eta}{y})R_1}] - \mathbb{E}[e^{(\sigma - \frac{1 - \eta}{y})R_2}] \geq \frac{\sigma^{1 - \eta}}{\Gamma(1 - \eta)} x_0^{-\eta} \frac{1}{(1 - \eta)/y} e^{-(1 - \eta)x_0/y} \frac{\sigma y - 1}{2(\sigma y + 1)(\sigma x_0 - 1)}.$$

Recalling $\Gamma(\alpha) \geq \Gamma(1 - \eta)$ and $x_0 \geq \frac{2}{\alpha}y \geq y$, and plugging the preceding display into the separation inequality (C.7), we have

$$\begin{aligned} |I_1 - I_2| &\geq \frac{1}{\Gamma(\alpha)} \left(\frac{y}{x_0(1 - \eta)} \right)^\eta e^{-(1 - \eta)x_0/y} \frac{\sigma y - 1}{2(\sigma y + 1)(\sigma x_0 - 1)} \\ &\geq \frac{1}{\Gamma(\alpha)} \left(\frac{y}{x_0} \right)^{1 - \alpha} e^{-(1 - \eta)x_0/y} \frac{\sigma y - 1}{2(\sigma y + 1)(\sigma x_0 - 1)}, \end{aligned}$$

where we used $(1 - \eta)^{-\eta} \geq 1$ in the final inequality.

C.2 Proof of Lemma 9

Using the bound (C.3), we have

$$\begin{aligned} D_{\text{kl}}(P_1 \| P_2) &= \int_{x_0}^{\infty} \frac{\sigma^{1 - \eta}}{\Gamma(1 - \eta)} x^{-\eta} e^{-\sigma x} \log \frac{\frac{\sigma^{1 - \eta}}{\Gamma(1 - \eta)} x^{1 - \eta}}{C} dx \\ &\leq \int_{x_0}^{\infty} \frac{\sigma^{1 - \eta}}{\Gamma(1 - \eta)} x^{-\eta} e^{-\sigma x} \log \frac{x^{1 - \eta}}{x_0^{1 - \eta} \left(1 - \frac{\eta}{\sigma x_0}\right)} dx \\ &\leq \int_{x_0}^{\infty} \frac{\sigma^{1 - \eta}}{\Gamma(1 - \eta)} x^{-\eta} e^{-\sigma x} \log \frac{x}{x_0 \left(1 - \frac{\eta}{\sigma x_0}\right)} dx \\ &= \frac{\sigma^{1 - \eta}}{\Gamma(1 - \eta)} \left[-\log \left(x_0 - \frac{\eta}{\sigma}\right) \int_{x_0}^{\infty} x^{-\eta} e^{-\sigma x} dx + \int_{x_0}^{\infty} x^{-\eta} e^{-\sigma x} \log x dx \right]. \end{aligned}$$

Integration by parts gives us

$$\begin{aligned} \int_{x_0}^{\infty} x^{-\eta} e^{-\sigma x} \log x dx &= \frac{x_0^{-\eta}}{\sigma} e^{-\sigma x_0} \log x_0 + \frac{1}{\sigma} \int_{x_0}^{\infty} e^{-\sigma x} x^{-\eta - 1} (1 - \eta \log x) dx \\ &\leq \frac{x_0^{-\eta}}{\sigma} e^{-\sigma x_0} \log x_0 + \frac{1}{\sigma} \int_{x_0}^{\infty} e^{-\sigma x} x^{-\eta - 1} dx \leq \frac{x_0^{-\eta}}{\sigma} e^{-\sigma x_0} \left(\log x_0 + \frac{1}{\sigma x_0} \right). \end{aligned}$$

Using $\log x \leq x - 1$ and the assumption $x_0 \geq 1 + \frac{1}{\sigma} \geq 1 + \frac{\eta}{\sigma}$,

$$\begin{aligned} \frac{\Gamma(1 - \eta)}{\sigma^{1 - \eta}} D_{\text{kl}}(P_1 \| P_2) &\leq -\frac{x_0^{-\eta}}{\sigma} e^{-\sigma x_0} \left(1 - \frac{\eta}{\sigma x_0}\right) \log \left(x_0 - \frac{\eta}{\sigma}\right) + \frac{x_0^{-\eta}}{\sigma} e^{-\sigma x_0} \left(\log x_0 + \frac{1}{\sigma x_0} \right) \\ &= \frac{x_0^{-\eta}}{\sigma} e^{-\sigma x_0} \log \frac{x_0}{x_0 - \eta/\sigma} + \frac{x_0^{-\eta}}{\sigma^2 x_0} e^{-\sigma x_0} \left(\eta \log \left(x_0 - \frac{\eta}{\sigma}\right) + 1 \right) \end{aligned}$$

$$\begin{aligned}
&\leq \frac{x_0^{-\eta}}{\sigma} e^{-\sigma x_0} \frac{\eta/\sigma}{x_0 - \eta/\sigma} + \frac{x_0^{-\eta}}{\sigma^2 x_0} e^{-\sigma x_0} \left(\eta x_0 - \frac{\eta^2}{\sigma} - \eta + 1 \right) \\
&\leq \frac{x_0^{-\eta}}{\sigma} e^{-\sigma x_0} \left(\frac{2\eta}{\sigma} + \frac{1}{\sigma x_0} \right) \leq 3 \frac{x_0^{\frac{1}{2}(\alpha-1)}}{\sigma^2} e^{-\sigma x_0}
\end{aligned}$$

where in the last step, we used the inequalities (C.1) and $\eta \in [0, 1]$. Using the inequalities (C.1) again and $\sigma^{-\eta-1} \leq 1 \vee \sigma^{-2}$, it follows that

$$D_{\text{kl}}(P_1 \| P_2) \leq 3 \frac{\sigma^{-\eta-1}}{\Gamma(1-\eta)} x_0^{\frac{1}{2}(\alpha-1)} e^{-\sigma x_0} \leq 3(1 \vee \sigma^{-2}) x_0^{\frac{1}{2}(\alpha-1)} e^{-\sigma x_0}.$$

Since $x_0 \geq \frac{\log 3(1 \vee \sigma^{-2})}{\frac{1}{2}(1-\alpha)}$, we have $D_{\text{kl}}(P_1 \| P_2) \leq e^{-\sigma x_0}$.

C.3 Proof of Theorem 6

As in Section C.1, we use Le Cam's method. Let $R_1 \sim P_1 = \text{Exp}(\sigma)$ with density $f_1(x) = \sigma e^{-\sigma x} \mathbf{1}\{x \geq 0\}$ and $R_2 \sim P_2$ with density

$$f_2(x) = \begin{cases} 0 & \text{if } x < 0 \\ \sigma(1+\omega)e^{-\sigma(1+\omega)x} & \text{if } 0 \leq x \leq x_0 \\ \sigma e^{-\sigma\omega x_0} e^{-\sigma x} & \text{if } x > x_0 \end{cases}$$

for some $x_0, \omega > 0$ to be chosen later. First, we show that both P_1 and P_2 are in $\mathcal{P}_{\sigma, y, \alpha}$.

Lemma 12. *For $\omega \leq \frac{1-\alpha}{\sigma y} \wedge \frac{2-\sigma y}{\sigma y}$, we have $P_1, P_2 \in \mathcal{P}_{\sigma, y, \alpha}$.*

See Section C.3.1 for the proof. Next, we prove that I_1 and I_2 are $\Omega(\omega)$ apart.

Lemma 13.

$$|I_1 - I_2| = I_2 - I_1 \geq \frac{\sigma y - 1}{\omega \sigma y + 1} (1 - e^{-(\sigma\omega + 1/y)x_0}) \omega.$$

Despite the rate functions being $\Omega(\omega)$ -separated, we next show that P_1 and P_2 are $O(\omega^2)$ -close in total variation distance. From Pinsker's inequality, we have $\|P_1^n - P_2^n\|_{\text{TV}}^2 \leq \frac{1}{2} D_{\text{kl}}(P_1^n \| P_2^n) = \frac{n}{2} D_{\text{kl}}(P_1 \| P_2)$. We have

$$\begin{aligned}
D_{\text{kl}}(P_1 \| P_2) &= \int_0^{x_0} \sigma e^{-\sigma x} \log \frac{\sigma e^{-\sigma x}}{\sigma(1+\omega)e^{-\sigma(1+\omega)x}} dx + \int_{x_0}^{\infty} \sigma e^{-\sigma x} \log \frac{\sigma e^{-\sigma x}}{\sigma e^{-\sigma\omega x_0} e^{-\sigma x}} dx \\
&= -\sigma\omega x_0 e^{-\sigma x_0} + \frac{1}{\omega} (1 - e^{-\sigma x_0}) - (1 - e^{-\sigma x_0}) \log(1+\omega) + \sigma\omega x_0 e^{-\sigma x_0} \\
&= (\omega - \log(1+\omega))(1 - e^{-\sigma x_0}) \leq \frac{1}{2} \omega^2 (1 - e^{-\sigma x_0}),
\end{aligned}$$

where we used $x - \log(1+x) \leq \frac{1}{2}x^2$ for all $x \geq 0$. Now, let $x_0 = \sigma^{-1} \log n$ and $\omega = \frac{c}{\sqrt{n}}$ for $c = 2(1 - 2\delta)$. Then, $D_{\text{kl}}(P_1 \| P_2) \leq \frac{1}{2} \omega^2$ so that $\|P_1^n - P_2^n\|_{\text{TV}} \leq \frac{c}{2}$. Since $x_0 \geq y \log 2$ and $\omega > 0$, we have $e^{-(\sigma\omega + 1/y)x_0} \leq \frac{1}{2}$ and $\frac{1}{\omega\sigma y + 1} \geq \frac{1}{2}$. From Lemma 13, we get $|I_1 - I_2| \geq \frac{\sigma y - 1}{4} \omega$. Using these two bounds in Lemma 6, we obtain $\mathfrak{M}_n \geq \delta$ as desired.

C.3.1 Proof of Lemma 12

Evidently, $P_1 \in \mathcal{P}_{\sigma,y,\alpha}$ since $\mathbb{E}e^{\lambda R_1} = \frac{\sigma}{\sigma-\lambda}$, $\mathbb{E}[R_1] = \frac{1}{\sigma}$, and $\lambda^*(P_1) = \sigma - 1/y$. To show $P_2 \in \mathcal{P}_{\sigma,y,\alpha}$, we first note that P_2 clearly satisfies Condition 1. Then we check Condition 2, which follows from

$$\begin{aligned}\mathbb{E}e^{\lambda R_2} &= \frac{\sigma(1+\omega)}{\sigma(1+\omega)-\lambda}(1 - e^{-(\sigma(1+\omega)-\lambda)x_0}) + \frac{\sigma}{\sigma-\lambda}e^{-(\sigma(1+\omega)-\lambda)x_0} \\ &= \frac{\sigma}{\sigma-\lambda} \left(1 - \frac{\omega\lambda}{\sigma(1+\omega)-\lambda}(1 - e^{-(\sigma(1+\omega)-\lambda)x_0}) \right) \leq \frac{\sigma}{\sigma-\lambda},\end{aligned}\quad (\text{C.8})$$

and

$$\mathbb{E}[R_2] = \int_0^{x_0} \sigma(1+\omega)x e^{-\sigma(1+\omega)x} dx + \int_{x_0}^{\infty} \sigma x e^{-\sigma\omega x_0} e^{-\sigma x} dx = \frac{1}{\sigma(1+\omega)}(1 + \omega e^{-\sigma(1+\omega)x_0}) \leq \frac{1}{\sigma}.$$

It remains to show Condition 3. Since $\omega \leq \frac{1-\alpha}{\sigma y}$, $\sigma(1+\omega) - \frac{1}{y} \leq \sigma - \frac{\alpha}{y}$, it suffices to show $\lambda^*(P_2) \leq \sigma(1+\omega) - 1/y$. Similar to inequality (3.2), we need to show $\mathbb{E}[R_2 e^{\lambda R_2}] \geq y \mathbb{E}[e^{\lambda R_2}]$ when $\lambda = \sigma(1+\omega) - \frac{1}{y}$. Plugging $\lambda = \sigma(1+\omega) - \frac{1}{y}$ into the preceding display (C.8), we obtain

$$\mathbb{E}[e^{(\sigma(1+\omega)-\frac{1}{y})R_2}] = \sigma(1+\omega)y \left(1 - e^{-x_0/y} \right) + \frac{\sigma}{\frac{1}{y} - \omega\sigma} e^{-x_0/y}.$$

Next, integration by parts gives

$$\begin{aligned}\mathbb{E}[R_2 e^{\lambda R_2}] &= \int_0^{x_0} \sigma(1+\omega)x e^{-(\sigma(1+\omega)-\lambda)x} dx + \int_{x_0}^{\infty} \sigma e^{-\sigma\omega x_0} x e^{-(\sigma-\lambda)x} dx \\ &= \frac{\sigma(1+\omega)}{\sigma(1+\omega)-\lambda} \left(-x_0 e^{-(\sigma(1+\omega)-\lambda)x_0} + \frac{1}{\sigma(1+\omega)-\lambda} (1 - e^{-(\sigma(1+\omega)-\lambda)x_0}) \right) \\ &\quad + \frac{\sigma}{\sigma-\lambda} e^{-\sigma\omega x_0} \left(x_0 e^{-(\sigma-\lambda)x_0} + \frac{1}{\sigma-\lambda} e^{-(\sigma-\lambda)x_0} \right).\end{aligned}$$

Plugging in $\lambda = \sigma(1+\omega) - \frac{1}{y}$ again, we have

$$\begin{aligned}\mathbb{E}[R_2 e^{(\sigma(1+\omega)-\frac{1}{y})R_2}] &= \sigma(1+\omega)y \left(-x_0 e^{-x_0/y} + y(1 - e^{-x_0/y}) \right) \\ &\quad + \frac{\sigma}{\frac{1}{y} - \omega\sigma} e^{-\sigma\omega x_0} \left(x_0 e^{-(\frac{1}{y}-\omega\sigma)x_0} + \frac{1}{\frac{1}{y} - \omega\sigma} e^{-(\frac{1}{y}-\omega\sigma)x_0} \right).\end{aligned}$$

Taking differences, we get

$$\begin{aligned}&\mathbb{E}[R_2 e^{(\sigma(1+\omega)-\frac{1}{y})R_2}] - y \mathbb{E}[e^{(\sigma(1+\omega)-\frac{1}{y})R_2}] \\ &= \frac{e^{-x_0/y} y \omega \sigma}{(1 - \sigma y \omega)^2} \left[x_0 \left(-1 - y^2 \omega (1 + \omega) \sigma^2 + y \sigma (1 + 2\omega) \right) + \sigma y^2 \right] \\ &\stackrel{(a)}{\geq} \frac{e^{-x_0/y} y \omega \sigma}{(1 - \sigma y \omega)^2} \left[x_0 \left(-1 - 2\omega \sigma y + y \sigma (1 + 2\omega) \right) + \sigma y^2 \right] \\ &\stackrel{(b)}{\geq} \frac{e^{-x_0/y} y \omega \sigma}{(1 - \sigma y \omega)^2} \sigma y^2 \geq 0\end{aligned}$$

where we used $1 + \omega \leq \frac{2}{\sigma y}$ in step (a) and $\sigma y \geq 1$ in step (b). We conclude that P_2 satisfies Condition 3.

C.3.2 Proof of Lemma 13

Plugging $\mathbb{E}[e^{\lambda R_1}] = \frac{\sigma}{\sigma - \lambda}$ into the expression for I_1 , we get $\lambda^*(P_1) = \sigma - \frac{1}{y}$ and

$$I_1 = \sup_{\lambda} \{\lambda y - \kappa_1(\lambda)\} = y(\sigma - 1/y) - \kappa_1(\sigma - 1/y).$$

Then, we have the following lower bound on the separation:

$$\begin{aligned} |I_1 - I_2| &\geq I_2 - I_1 = \sup_{\lambda} \{\lambda y - \kappa_2(\lambda)\} - \sup_{\lambda} \{\lambda y - \kappa_1(\lambda)\} \\ &\geq y(\sigma - 1/y) - \kappa_2(\sigma - 1/y) - (y(\sigma - 1/y) - \kappa_1(\sigma - 1/y)) \\ &= \kappa_1(\sigma - 1/y) - \kappa_2(\sigma - 1/y) = \log \frac{\mathbb{E}e^{(\sigma-1/y)R_1}}{\mathbb{E}e^{(\sigma-1/y)R_2}} \\ &\geq \frac{\mathbb{E}e^{(\sigma-1/y)R_1} - \mathbb{E}e^{(\sigma-1/y)R_2}}{\mathbb{E}e^{(\sigma-1/y)R_1}} = \frac{1}{\sigma y} \left(\mathbb{E}[e^{(\sigma-1/y)R_1}] - \mathbb{E}[e^{(\sigma-1/y)R_2}] \right) \end{aligned} \quad (\text{C.9})$$

where we have used $\log x \geq 1 - \frac{1}{x}$ in the last inequality. Using previous calculations (C.8),

$$\mathbb{E}[e^{\lambda R_1}] - \mathbb{E}[e^{\lambda R_2}] = \frac{\sigma \omega \lambda}{(\sigma - \lambda)(\sigma(1 + \omega) - \lambda)} (1 - e^{-(\sigma(1+\omega) - \lambda)x_0}).$$

Plugging in $\lambda = \sigma - 1/y$, we obtain

$$\mathbb{E}[e^{(\sigma-1/y)R_1}] - \mathbb{E}[e^{(\sigma-1/y)R_2}] = \sigma y \frac{\sigma y - 1}{\omega \sigma y + 1} (1 - e^{-(\sigma\omega + 1/y)x_0}) \omega.$$

Plugging this in (C.9), we get the desired result.

C.4 Proof of Corollary 2

Let $P_1 = \mathcal{N}(y - \bar{\lambda}, 1)$ and $P_2 = \mathcal{N}(y - \bar{\lambda} + \frac{c}{\sqrt{n}}, 1)$ with $c = 2(1 - 2\delta)$. From Example 1, we have

$$\begin{aligned} \lambda_y^*(P_1) &= \bar{\lambda} \\ \lambda_y^*(P_2) &= \bar{\lambda} - \frac{c}{\sqrt{n}} < \bar{\lambda}, \end{aligned}$$

so that $P_1, P_2 \in \mathcal{Q}_{\bar{\lambda}, y}^-$.

It is straightforward to verify that

$$D_{\text{kl}}(P_1 \| P_2) = \frac{c^2}{2n},$$

and

$$\begin{aligned} I_1 &= \frac{1}{2}(\bar{\lambda})^2, \\ I_2 &= \frac{1}{2} \left(\bar{\lambda} - \frac{c}{\sqrt{n}} \right)^2, \\ |I_1 - I_2| &= \frac{c}{\sqrt{n}} \bar{\lambda} - \frac{1}{2} \frac{c^2}{n} \geq \frac{c}{2\sqrt{n}} \bar{\lambda}, \end{aligned}$$

where the last inequality follows from the assumption $n \geq \left(\frac{c}{\bar{\lambda}}\right)^2$ so that $\frac{c^2}{n} \leq \frac{c}{\sqrt{n}} \bar{\lambda}$. From Pinsker's inequality, we have $\|P_1^n - P_2^n\|_{\text{TV}}^2 \leq \frac{1}{2} D_{\text{kl}}(P_1^n \| P_2^n) = \frac{n}{2} D_{\text{kl}}(P_1 \| P_2) = \frac{c^2}{4} = (1 - 2\delta)^2$. Applying Lemma 6, we obtain $\mathfrak{M}_n \geq \delta$ as claimed.

D Experimental details

D.1 Details of the DQN model for queueing

The DQN model is implemented in OpenAI Gym [18], a toolkit for benchmarking reinforcement learning algorithms, to build our discrete-event simulator. Using our custom simulator, the queueing process can be modeled as a Markov Decision Process \mathcal{M} as follows.

- Time steps t are time points when the scheduler needs to make decisions.
- The state s_t is history information up to step t . As we allow non-exponential arrival distributions, we need all history information as the state. Even though one can use a recurrent neural network [70] to parametrize the Q function and use s_t directly, here we opt for a simpler approach similar to [109]: use a preprocessing function $\Phi(\cdot)$ to compress state information into a low-dimensional vector ϕ_t and update Q through ϕ_t instead of s_t . Based on domain knowledge of queueing systems, we choose ϕ_t as a vector concatenating queue length and age of the oldest job for each type of job at step t . Thus, $\phi_t \in \mathbb{N}^3 \times \mathbb{R}_+^3$. Using x_t to denote information between step $t - 1$ and step t , we have $s_t = s_{t-1}, x_t$. This is consistent with notations in [109].
- The action $a_t \in \{1, 2, 3\}$ represents the queue that the server chooses to serve.
- We assume initially there is one job in each queue, so the system needs to make a decision initially.
- The transition probability is specified by the simulator.
- The reward function is $r_a(\phi_t, \phi_{t+1}) = -(1, 3, 6)^\top \cdot \text{age}(\phi_{t+1}) - 1,000,000 \cdot \mathbb{I}(\text{if the queue for type } a \text{ is empty at step } t)$ where $\text{age}(\phi_{t+1})$ is the age part of vector ϕ_{t+1} . The large cost associated with the selection of empty queues is introduced to dissuade the model from making such suboptimal decisions. We choose this reward function based on experimental results and inspired by [103].
- To deal with the unboundedness of the state space, we implement policy π_0 : FIFO when one of the queue lengths is larger than the threshold $G = 10$. In the algorithm, we use $g(\phi_t)$ to represent the largest queue length at step t .
- We apply a pure exploration strategy and do not update the Q function in the first half of episodes; this is observed to help stabilize training in our experiment.
- We also use experience replay [101], a buffer with fixed size storing most recent transitions and rewards information, which is a central tool in deep reinforcement learning to improve sample efficiency.

To approximate the action-value function Q , we use Pytorch [115] to construct a fully connected feedforward neural network with two hidden layers with ReLU activation functions. The numbers of units for each layer are 6, 4, 4, 3, respectively. Here, we use θ to denote the weights and biases of the neural network. The parameters θ are initialized by standard Kaiming initialization [71]. More details of our method are given in Algorithm 1, and hyperparameters are summarized in Table 2.

Algorithm 1 Deep Q-learning with Experience Replay for Queueing Systems Control

```
1: Initialize replay memory  $\mathcal{D}$  to an empty double-ended queue with size  $N$ 
2: Initialize the action-value function  $Q$ 
3: for episode = 1 to  $M$  do
4:   Initialize  $s_1 = x_1$ , and  $\phi_1 = \Phi(s_1)$ 
5:   for  $t = 1$  to  $T$  do
6:     Sample  $U \sim \text{Uniform}[0, 1]$ 
7:     if  $U \leq \epsilon$  or episode  $\leq M/2$  then
8:       Randomly select  $a_t$ 
9:     else if  $g(\phi_t) \geq G$  then
10:      Select  $a_t$  based on  $\pi_0$ 
11:     else
12:      Select  $a_t = \operatorname{argmax}_a Q(\phi_t, a; \theta)$ 
13:     end if
14:     Execute action  $a_t$ , observe  $x_{t+1}$ 
15:     Update  $s_{t+1} = s_t, x_{t+1}$  and  $\phi_{t+1} = \Phi(s_{t+1})$ 
16:     Compute  $r_t = r_{a_t}(\phi_t, \phi_{t+1})$ 
17:     Append  $(\phi_t, a_t, r_t, \phi_{t+1})$  to  $\mathcal{D}$ 
18:     if episode  $> M/2$  then
19:       Sample a batch  $\mathcal{B}$  with size  $B$  from  $\mathcal{D}$ 
20:       For every  $j \in \mathcal{B}$ , set  $q_j = r_j + \gamma \max_a Q(\phi_{j+1}, a; \theta)$ 
21:       Use the optimizer on  $\sum_{j \in \mathcal{B}} \ell(q_j; Q(\phi_j, a_j; \theta))$  to update  $\theta$ 
22:     end if
23:   end for
24: end for
```

Hyperparameter	Value
Number of episodes M	40
Number of steps per episode T	30,000
Replay memory capacity N	1,000
Replay memory sample size B	100
Exploration probability ϵ	0.05
Discounting factor γ	0.9
Loss function $\ell(\cdot; \cdot)$	Huber loss with parameter $\delta = 1$
Optimizer	Adam optimizer [84] with $(\beta_1, \beta_2) = (0.9, 0.999)$, learning rate 0.01, $\epsilon = 10^{-8}$, and weight decay 0.001

Table 2: Hyperparameters for DQN

D.2 Details of the Health utilization prediction models

Variable	Meaning
sex_female	If the individual is female or not
educ_yrs	Years of education
health_status_excellent	If the health status is excellent
wrkhrs	Working hours per week
overnight_hospital_times	Times of visiting hospital overnight
care_athome_2wks_times	Number of home visits by health professionals in 2 weeks
looking_for_work	If the individual is looking for work
not_work_health	Main reason for not working last week: due to health
care_10more_12mo	Received care 10+ times in the last 12 months
wrk_mo_lastyr	Months worked last year
limited_any_lt5	Any limitation - all persons, all conditions
overnight_hospital_nights	Nights of visiting hospital overnight
hikind_nocov	No coverage of any type
care_spent_zero	Amount family spent for medical care
hino_months	Months without coverage in the past 12 months
health_status_fair	Reported health status as fair

Table 3: Core variables

Since typical ML training algorithms output classification probabilities (estimates of $\mathbb{P}(Y = 1|X)$) that are poorly calibrated [69], we explicitly adjust these estimators using a constant finetuned on a small held-out data, a standard post-processing process known as “model calibration” [112]. In Algorithm 2, we construct the partition S_1, \dots, S_4 by randomly splitting the entire 2015 data into 80%, 10%, 5%, 5% subsets respectively. For simplicity, we always use a random forest classifier for the auxiliary model class \mathcal{H} . Since all classifiers are trained on S_1 , we use $S_2 \cup S_3 \cup S_4$ to evaluate the average accuracy of each model.

Algorithm 2 Estimate stability for prediction models

- 1: INPUT: Partition of samples S_1, S_2, S_3, S_4 , prediction model class \mathcal{F} , auxiliary class \mathcal{H}
 - 2: Fit a classifier $f(X) \in \mathcal{F}$ to predict Y using data S_1 .
 - 3: Calibrate f using data S_2 .
 - 4: Fit $h(Z) \in \mathcal{H}$ to predict $\ell(f(X); Y)$ based on core variables Z using data S_3 .
 - 5: Compute the plug-in stability estimator \hat{I}_n of $h(Z)$ over data in S_4 .
-

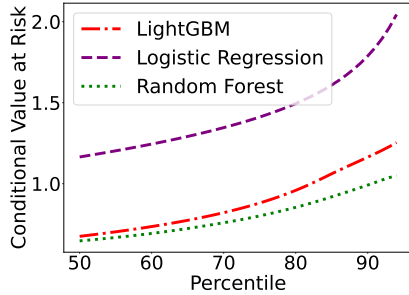


Figure 18. CVaR with quantile level α for the cross-entropy loss for different models

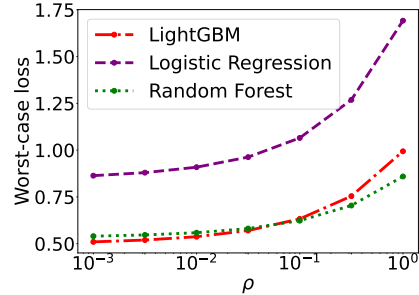


Figure 19. Worst-case expectation over a KL neighborhood of radius ρ for the cross-entropy loss for different models

Variable	Meaning
sex_female	If the individual is female or not
medicaid_	If uses Medicaid or not
educ_yrs	Years of education
health_status_excellent	If the health status is excellent
wrkhrs	Working hours per week
overnight_hospital_times	Times of visiting hospital overnight
care_athome_2wks_times	Number of home visits by health professionals in 2 weeks
looking_for_work	If the individual is looking for work
not_work_retired	If the individual retired

Table 4: New core variables

To compare the stability measure with other risk measures, we apply CVaR on the cross-entropy loss of three models. In Figure 18, CVaR of the cross-entropy loss predicts that LightGBM is much more stable than Logistic Regression, which is quite the opposite of what we see in Section 5.2. Similarly, in Figure 19, we estimate the worst-case expectation using (A.4) and we observe that this metric applying on the cross-entropy loss does not predict the stability ranking well. In addition, in Figures 20 and 21, we estimate the worst-case expectation and CVaR for the conditional risk (5.1). We observe that when applying on the conditional risk, traditional risk measures also successfully predict the robustness of each model. This again underscores the significance of choosing a proper performance measure R .

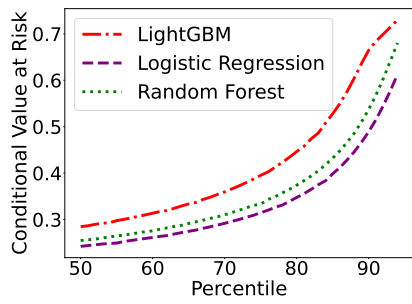


Figure 20. CVaR with quantile level α for the conditional loss (5.1) for different models

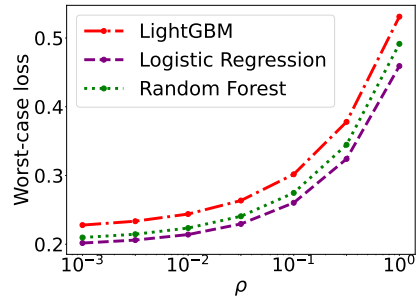


Figure 21. Worst-case expectation over a KL neighborhood of radius ρ for the conditional loss (5.1) for different models